AD_____

Award Number: DAMD17-02-2-0011

TITLE: Structural Studies on Intact Clostridium Botulinum Neurotoxins Complexed with Inhibitors Leading to Drug Design

PRINCIPAL INVESTIGATOR: Subramanyam Swaminathan, Ph.D.

CONTRACTING ORGANIZATION: Brookhaven National Laboratory
Upton, New York 11973

REPORT DATE: February 2005

TYPE OF REPORT: Annual

PREPARED FOR: U.S. Army Medical Research and Materiel Command
Fort Detrick, Maryland 21702-5012

REPORT DOCUMENTATION PAGE

Form Approved
OMB No. 074-0188

1. AGENCY USE ONLY (Leave blank)	2. REPORT DATE	3. REPORT TYPE AND DATES COVERED
	February 2005	Annual (28 Jan 04 - 27 Jan 05)

4. TITLE AND SUBTITLE
Structural Studies on Intact Clostridium Botulinum Neurotoxins Complexed with Inhibitors Leading to Drug Design

5. FUNDING NUMBERS
DAMD17-02-2-0011

6. AUTHOR(S)
Subramanyam Swaminathan, Ph.D.

7. PERFORMING ORGANIZATION NAME(S) AND ADDRESS(ES)
Brookhaven National Laboratory
Upton, New York 11973

E-Mail: swami@bnl.gov

8. PERFORMING ORGANIZATION REPORT NUMBER

9. SPONSORING / MONITORING AGENCY NAME(S) AND ADDRESS(ES)
U.S. Army Medical Research and Materiel Command
Fort Detrick, Maryland 21702-5012

10. SPONSORING / MONITORING AGENCY REPORT NUMBER

11. SUPPLEMENTARY NOTES

12a. DISTRIBUTION / AVAILABILITY STATEMENT
Approved for Public Release; Distribution Unlimited

12b. DISTRIBUTION CODE

13. ABSTRACT (Maximum 200 Words)

In this third annual report we present our progress on two different areas. We have identified two ganglioside binding sites in tetanus toxin. While one is common to botulinum toxins, the other is unique for tetanus. The second unique site also binds a tri-peptide which suggests that this peptide could be used as an inhibitor for tetanus, at least. We have determined the structure of the C fragment of botulinum neurotoxin type B. We have identified a number of inactive mutants of BoNT/E-LC. Some of these mutants may be potential candidates for vaccines. Most importantly, for the first time we have shown that Glu335Gln mutant of BoNT/E-LC is an apoenzyme devoid of zinc.

14. SUBJECT TERMS
Clostridium, botulinum, neurotoxin, zinc chelators, inhibitors, macromolecular crystallography, 3D structure

15. NUMBER OF PAGES
54

16. PRICE CODE

17. SECURITY CLASSIFICATION OF REPORT	18. SECURITY CLASSIFICATION OF THIS PAGE	19. SECURITY CLASSIFICATION OF ABSTRACT	20. LIMITATION OF ABSTRACT
Unclassified	Unclassified	Unclassified	Unlimited

Table of Contents

Structural Studies on Intact *Clostridium botulinum* Neurotoxins Complexed with Inhibitors Leading to Drug Design
Annual Report for the Period ending January 2005

Introduction

The overall goal of this project is to identify small molecules or peptides that will inhibit the toxicity of botulinum neurotoxins. Inhibition of toxicity of botulinum toxins can be achieved by blocking one of the four stages of toxicity – binding to neuronal cell, internalization into the vesicle, translocation into the cytosol and the catalytic activity of the light chain. In this project we are concentrating on two targets – the binding domain and the catalytic domain. The binding of neurotoxin is thought to be via two receptors – low affinity gangliosides and high affinity protein receptors. While the binding site of ganglioside is fairly well defined, neither the protein receptor nor its binding site is yet defined. Accordingly, we are attempting to block ganglioside binding site of the neurotoxins. The second target is the catalytic domain. The catalytic domain acts as a zinc endopeptidase. A two-pronged approach is being used. We are trying either small molecules which could chelate the active-site zinc or peptide mimics of the substrates to block the active site residues. The general approach is to study the crystal structure of the toxin in complex with a potential inhibitor via x-ray crystallography and then analyze the interactions between the inhibitor and the protein.

Body

(1) Structural analysis of C. neurotoxins in complex with molecules binding to the C-terminal domain of C. neurotoxin

(a) In the last annual report, we had reported the progress on our work on tetanus neurotoxin C-fragment. Botulinum neurotoxins and tetanus neurotoxin share significant sequence homology and are therefore expected to have similar three-dimensional structures. The experimental models of the C-fragment of tetanus toxin and the C-terminal domain of botulinum neurotoxins have similar structure except for the loop

regions. The cavity at the sugar-binding site which was defined in BoNT/B (1) is similar to the cavity present in the C-fragment of tetanus toxin (rTTC) (2). Based on this, it is reasonable to hypothesize that molecules that mimic Gt1b will bind in the same place in tetanus toxin and botulinum toxins. We have proved this in a few cases. We have completed the structural work on tetanus toxin in complex with disialyllactose which forms one branch of Gt1b sugar, a receptor for neurotoxins and a tripeptide which has been identified by docking studies. This paper has been accepted for publication in Proteins. A PDF file of the accepted manuscript is attached (Appendix 1).

(b) Crystal structure of the C-fragment of botulinum neurotoxin type B:

In the course of our work on tetanus toxin complexes with sugar molecules we discovered that while tetanus has two binding sites for ganglioside sugars, botulinum has only one. Or, two gangliosides can bind to a tetanus molecule simultaneously while only one can bind to botulinum. Of these two, one site is common to both tetanus and botulinum (Fig. 1). Site 1 is the ganglioside-binding site in botulinum. Both sites (1 and 2) are used in tetanus.

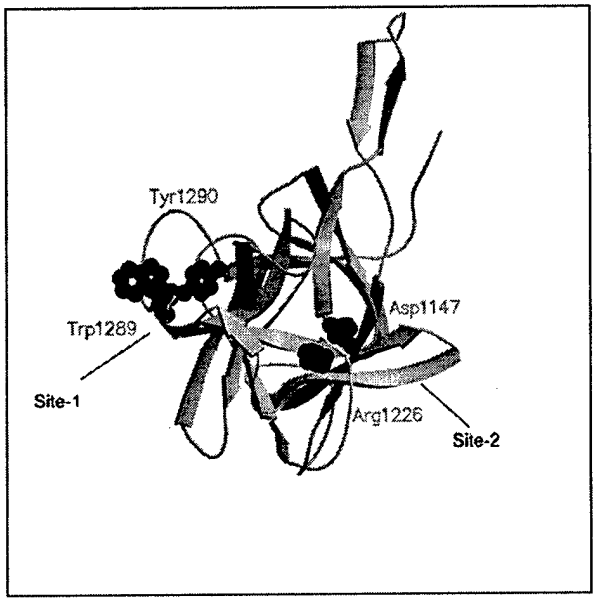

Fig.1

We are now extending our structural work to the C-fragment of botulinum neurotoxin type B (BBHc) to analyze this difference and effectively to use the information to identify molecules specific to each and generic to both.

BBHc containing residues 853-1290 of *Clostridium botulinum* type B, Danish strain was expressed from a synthetic gene in *Pichia pastoris*, and purified as described. The purified protein was supplied by Dr. Len Smith of USAMRIID. The protein was crystallized with Hampton Research Crystal screen. Good diffracting crystals were obtained using 60–100 mM ammonium formate and 30% PEG 6000 as precipitant. The crystal quality was improved further using the additive Sulfo-betaine 201. Rod-shaped

crystals of dimension 0.05 x 0.06 x 0.08 mm appeared after a week and diffracted to 1.9 Å. Crystals are in space group $P2_1$ with cell dimensions a = 68.47, b = 78.60, c = 87.85 and $\beta = 102.97°$ with two molecules in the asymmetric unit. . The two molecules in the asymmetric unit are related by a two-fold at ¼ along c-axis, parallel and halfway between crystallographic two-fold screws. Data were collected at liquid nitrogen temperature at X25 beam line of the NSLS, Brookhaven National Laboratory with a Q315 detector.

The structure was determined by the molecular replacement method using the poly-alanine model of the binding domain of BoNT/B structure (PDB id: 1ERW) as the search model (3). Loops were truncated in the model to avoid model bias. After initial rigid body refinement, side chains were included in the model. The model was refined by slow cool simulated annealing method with CNS and in each step, 2Fo-Fc and Fo-Fc maps were calculated to check and improve the model in the density maps using the program O (4). Cycles of rebuilding and refinement were continued until the convergence of R-factor and R-free. A total of 430 water molecules were located from the difference Fourier maps and were included in subsequent rounds of refinement. The model is complete except for 1150-1156 loop region.

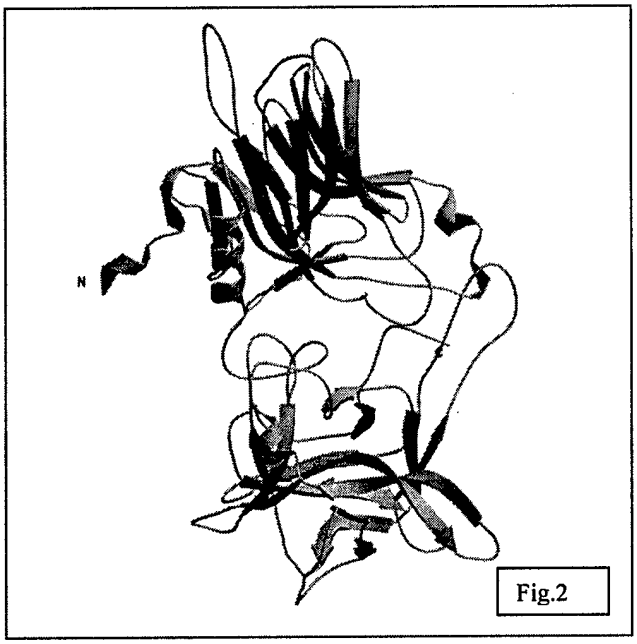

Fig.2

The structure of the BBHc is very similar to the C-fragment of tetanus toxin (Fig. 2). The overall structure of BBHc is well ordered and globally similar to that of the binding domain of the holotoxin structure except for the orientation of two loops located on the surface of the molecule and the N-terminal helix. The binding domain and the rest of the holotoxin are linked through the N-terminal α-helix of the binding domain. In the holotoxin structure the binding domain is tilted away from the central translocation domain and makes minimal contact with it. The two domains interact *via* nine hydrogen

bonds. There are 13 other possible hydrophilic contacts within 4.8 Å. Water molecules in the interface play an important role in binding these domains. In addition, numerous hydrophobic contacts are observed between the two domains involving the N-terminal helix and the loop at the interface (aa 911-924). The separation of binding domain causes the loss of these interactions resulting in major loop movements.

Comparison of the isolated binding domain and the binding domain of holotoxin revealed that there were some movements of the loops and the N-terminal helix. Overall, one loop in the N-terminal domain and two loops in the C-terminal domain show significant displacements. (i) In the holotoxin the N-terminal helix (aa 846-856) of binding domain is close and almost orthogonal to long helices in the translocation domain and makes extensive contacts with the translocation domain helices. The N-terminal helix bridges the two domains. After the domain separation it looses all its interactions and moves 19.5 Å away from its position changing its orientation. (ii) The loop (aa 911-924) at the interface of translocation and binding domain which makes direct hydrogen bonds with the translocation domain is displaced by 14.7 Å in the absence of these interactions. The buried hydrophobic residues at this region are exposed in BBHc. The solvent accessibility of the loop in the absence of translocation domain increases. (iii) One of the loops in the C-terminal region (aa 1245-1250) moves away from its position by 7.5 Å. This region binds sialyllactose and doxorubicin in the cleft between His1240 and Trp1261. Though the extended loop shows a displacement, the binding pocket which is at the beginning of the loop region maintains its shape and size. This loop movement may not affect any binding in this region.

The structure of BBHc shows that the separation of binding domain from the rest of holotoxin results in the large displacements of the loop and the N-terminal helix connecting the translocation and binding domains. This is probably the reason why the C-fragment is a very poor competitor of the toxin for receptor binding. There are no significant changes in the ganglioside-binding site between BBHc and BoNT/B binding domain and it is possible to use BBHc structure for determining complex structures to identify inhibitors for the binding domain. It is our endeavor to use this structure to identify more sugar molecules that will bind at the ganglioside-binding site of botulinum toxin.

(2) Studies with C. neurotoxin type E catalytic domain

In the last annual report we had reported our progress on expressing BoNT/E catalytic domain and its structure determination (Fig. 3). A paper has been published on the crystal structure of the light chain and a PDF file is attached (Appendix 2). Since this is a high-resolution structure, it will be used for identifying inhibitors.

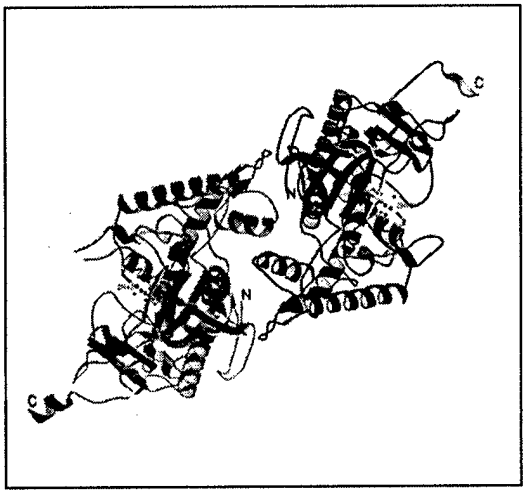

Fig. 3. Ribbons representation of BoNT/E-LC dimer. The two monomers are in green and blue. The active site zinc and the coordinating protein residues are in ball and stick model.

(a) Mutants of BoNT/E-LC:

We have done extensive work on the mutants of BoNT/E-LC. A number of mutants have been cloned, expressed and the activity tested. This was carried out for two reasons. (1) To identify residues that are important for the catalytic activity and then design inhibitors to block these residues, and (2) to understand the importance of each residue for the activity and thereby creating a mutant which would invoke the same antibody response but will be unable to cleave the substrate. Such a mutant may eventually be a valuable and potential candidate for vaccine development. Comparison of the region surrounding the active site of BoNT/E-LC with other serotypes revealed that many residues are conserved both in primary sequence and in three-dimensional space.

Since the interactions also were similar, it was hypothesized that the effect of mutating each of these residues will be the same for all serotypes (5). Accordingly, we have systematically mutated one residue at a time or in combination, analyzed the activity and determined their structures to study conformational changes, if any. The results are presented below.

Mutant BoNT/E-LC (Glu212Gln): The active site zinc ion is coordinated to Glu212 via a nucleophilic water molecule. Glu212 is thought to be responsible in shuttling/transferring two protons to the leaving group after the cleavage and accordingly mutating this to a neutral amino acid will block the activity. The crystal structure of the mutant is very similar to the wild-type structure. Overall, there is no conformational change and the secondary structural elements are the same. The only difference between the wild type and the mutant is the substitution of Glu with Gln at 212 (Fig. 4). Though the side chain orientation of Gln and Glu are very similar, there is no hydrogen bond interaction between Gln 212 OE1 or NE2 (distances >3.5 Å) thereby increasing the distance between zinc and the nucleophilic water to 2.8 Å from 2.2 Å in the wild type. This water molecule (which is not a nucleophilic water anymore) is stabilized by a network of water molecules leading up to Glu 158. The charge distribution at the active sites of both wild-type (left) and mutant structures (right) is presented in Figure 5. Since there is no change in the

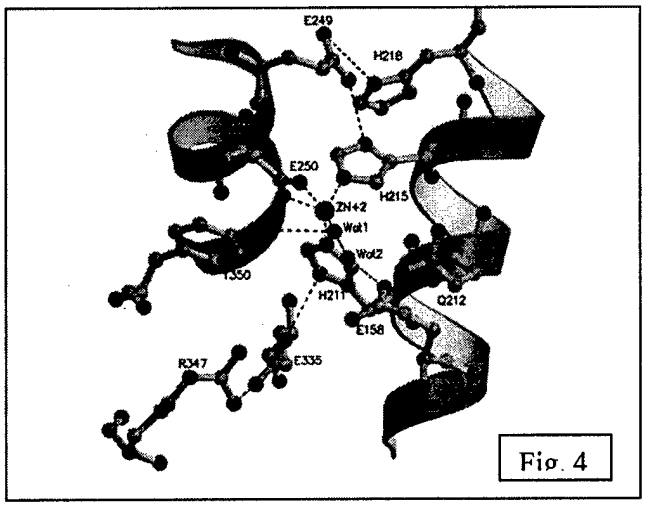

Fig. 4

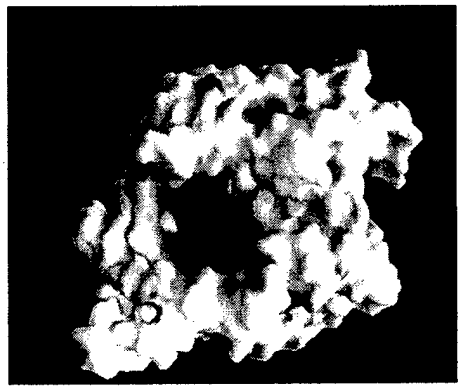

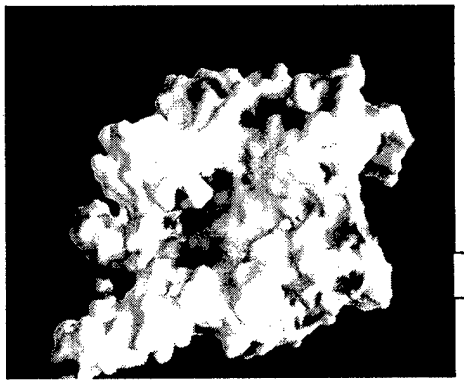
Fig. 5

structural features, the inductive effects exerted by the carboxylate side chain of Glu 212 in the wild-type L chain on neighboring groups must be responsible for the pronounced negative surface charge in the periphery of the active site. In other words, the neutralizing effect of the amide group of Gln 212 may be responsible for the decreased negative surface charge. In any case, it is evident that the change in the charge on Glu/Gln disturbs the electrostatic properties of the molecule at the active site inactivating the toxin.

This study supports the fact that a substitution of the Glu212 by Gln212 in the active site leads to the loss of the enzymatic activity of the protein. Structural data suggests that the loss in activity of the protein has not been the result of folding variation but due to the close involvement of the negative charge of carboxylate group which directly participates in the hydrolysis of the substrate. The distance and the topographical positioning of the carboxylate group play an essential role in the substrate hydrolysis (5). Please see the attached reprint.

Mutant BoNT/E-LC (Arg347Ala): Arg347 was selected for the study since this residue has been implicated in catalytic activity both by mutagensis study (BoNT/A) and by similarity to thermolysin Arg203 (6). In BoNT Arg347 is in the secondary coordination sphere. Glu335 acts as a bridge between Arg347 and His211 and is hydrogen bonded to them stabilizing the active site. It is possible that any perturbation in this interaction might affect the activity and the active site architecture. However, the terminal amide groups of Arg347 are more than 7Å away from either zinc or nucleophilic water in BoNTs. The active site geometry is almost preserved in Arg347Ala mutant structure. The coordination of zinc remains the same except for the nucleophilic water which has moved away to 2.6 Å changing from coordination to hydrogen bonding distance (Fig. 6). It was expected that the loss of hydrogen bonding interaction between Arg347 and Glu335 would affect the hydrogen bond contact between Glu335 and His211. However, this

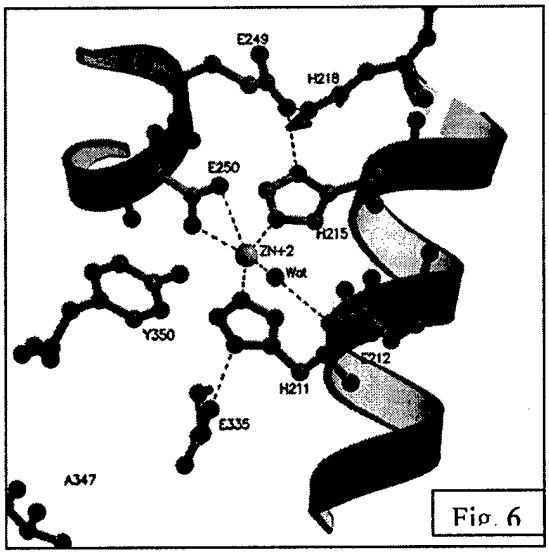

Fig. 6

hydrogen bond is intact and the orientation of His211 is unaltered and similar to that of the wild type structure.

Mutant BoNT/E-LC (Tyr35-Ala): Mutation of residue equivalent to Tyr350 has been studied both in BoNT/A and TeNT (6,7). When it was substituted with Phe, there was residual activity (25 to 30%) in both BoNT/A and TeNT. Mutation with Ala had different effects in BoNT/A and TeNT. While the activity was completely lost in TeNT, about 30% was retained in BoNT/A. In BoNT/E-LC the effect is similar to that of TeNT and the activity is barely detectable even at high concentration (5 μM) of the mutant enzyme (Tyr350Ala).

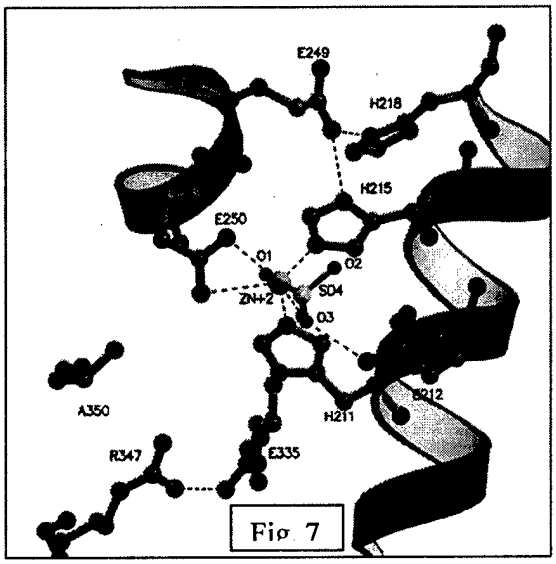

Fig. 7

As in the case of Arg347Ala, the conformation of the active site remains almost the same. The coordination distance between zinc and histidines are not changed. However, as a consequence of the loss of the phenolic ring and hence the aromatic-anion interaction stabilizing the position of Glu250, the side chain of Glu250 takes a different rotamer position and moves closer to the original position of Tyr350 side chain. It also increases the distance between zinc and the carboxylate group of Glu250 (molecule A). Interestingly, in the crystal structure of Tyr350Ala a sulfate ion replaces the nucleophilic water in molecule A similar to that observed in BoNT/B holotoxin structure. The presence of sulfate ion suggests that it has been incorporated during crystallization, since ammonium and lithium sulfates were present in the crystallization condition (Fig. 7).

The nucleophilic water is intact in molecule B of the LC dimer, though displaced to 3.21 Å from zinc. It moves closer to Glu212 and is at a distance of 2.42 Å making a very strong hydrogen bond. This is similar to movement of the water during transition state allowing the scissile carbonyl carbon to form a tetrahedral geometry. This movement of water closer to Glu212 is because of the loss of interaction between Tyr350 OH and the nucleophilic water that was present in the wild-type structure. This may be

one reason why a sulfate ion is able to displace the water in molecule A of Tyr350Ala unlike other BoNT/E structures where the water is tightly kept in position by tyrosine even though the crystallization conditions are same. The packing consideration could have prevented the replacement of water in molecule B.

Mutant BoNT/E-LC (Glu335Gln): Interestingly, when Glu was replaced by Gln (Glu335Gln) there was a drastic drop in catalytic efficiency (~7000-fold). Though the active site geometry remained the same, it was devoid of zinc (Fig. 8). Glu335 makes hydrogen bonds with Arg347 and His211 in the wild-type structure. Though the type of contacts may be different, Gln335 also makes hydrogen bonds with both Arg347 and His211 (significantly larger than wild type), but the orientation of His211 has changed ($\chi 2$ by 20°), and probably its protonation state also. It is intriguing that the nucleophilic water is still present, though moved away from the original position by about 0.8 Å (Fig. 8). It makes stronger hydrogen bonds with His215, Glu250 and Glu212 and also with the Tyr350. This suggests that the nucleophilic water is compensating for the loss of the zinc ion by interacting more closely with these residues.

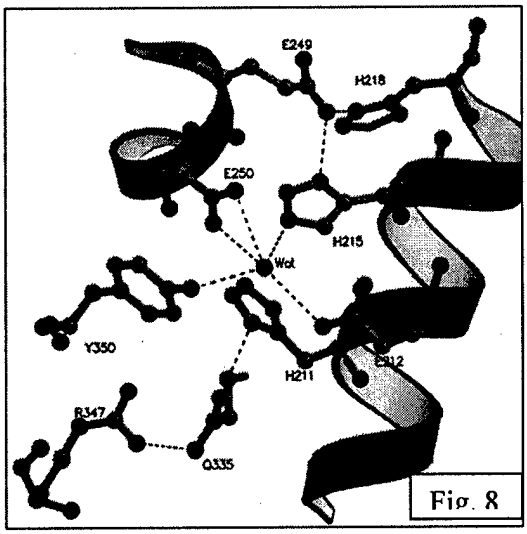

Fig. 8

Glu335Gln is an apoenzyme: In spite of the absence of zinc, there was some residual cleavage at high concentration (500 nm) of the mutant enzyme. It is not clear how a zinc endopeptidase devoid of zinc could still have some residual activity. One explanation is that the presence of nucleophilic water and its strong hydrogen bonding interactions could still help in attacking the carbonyl carbon of the scissile bond. Or, Glu212 which is strongly hydrogen bonded to the nucleophilic water could still act as a base, polarize the nucleophilic water and attack the carbonyl carbon without the help of zinc ion. This is similar to Glu144Ser active site mutant of the *Bacillus cereus* thermolysin like neutral protease where albeit the absence of a charged base some residual activity was detected and attributed to the nucleophilic water molecule strongly hydrogen bonded to Ser144, a neutral amino acid (8). However, while the zinc was still present in that structure, it is

absent in Glu335Gln. Another explanation for the residual activity could be the presence of traces of zinc in the assay buffer solutions which we rule out since ion free HPLC grade water was used in the assay buffer. In view of this Glu335Gln, an enzyme without the cofactor zinc, should be considered an apoenzyme – a persistent one in that since it cannot bind zinc anymore. Even though, we have shown that Glu212Gln is completely inactive, we constructed a double mutant Glu212Gln/Glu335Gln which will be an apoenzyme and inactive as well. As expected, this double mutant had no activity whatsoever.

The extremely low catalytic efficiency (~7000-fold less) shown by the mutation Glu335Gln along with it being an apoenzyme (devoid of zinc) is baffling. The data is also supported by similar biochemical results shown in BoNT/A-LC that mutating this residue to Ala/Gln led to drastic loss of activity and lowering of zinc content. The lower thermal stability observed in BoNT/A for this mutation may be due to the loss of zinc. Lowering of thermal stability has also been observed for apo BoNT/A-LC. When Glu is changed to Gln, the net charge changes by 1. This affects both the attractive and repulsive forces with the neighboring residues. Since the total electrostatic potential at any point is due to the sum total of all these changes, the environment must have changed. The change of interaction between this residue and the acidic residues would have caused this change. This is a classic example of how a subtle change in electrostatic properties (Glu is charged while Gln is neutral) can cause major change in the environment. When the electrostatic potential surfaces of the wild-type enzyme is compared to those of mutant structures it was clear that the electrostatic potential near Gln335 has changed considerably.

Conclusions from mutant study:

The present study reveals the role of the nucleophilic water and the charge on Glu212/Glu3335 on the catalytic activity. It also provides a method of developing a novel genetically-modified-protein vaccine. It suggests that a sensitive inhibitor could be developed if Glu212/Glu335 is blocked or covalently modified and may well become a common drug for all serotypes. Also, since they are spatially not far apart, it should be possible to design an inhibitor which will block both by interacting with both of them. Since the conformation of the mutant is almost identical to the wild-type protein and it

effectively binds to the substrate, the mutants offer themselves as candidates for studying the enzyme-substrate complex without the substrate being cleaved.

Key Research Accomplishments

- Two small molecules have been identified which may help in designing molecules to block gangliosides binding to C. neurotoxin.
- The same molecules also provide a model for ganglioside binding to neurotoxins.
- Residues vital for catalytic activity of BoNT/E have been identified by mutational and structural studies.
- Blocking one of the four residues, Glu212, Glu335, Arg347 and Tyr350 with small molecules will effectively inhibit the toxicity.
- This is first time it has been shown that Glu335Gln is an apoenzyme devoid of zinc.
- A few potential vaccine candidates have been identified.

Reportable outcomes

1. Rakhi Agarwal, S. Eswaramoorthy, D. Kumaran, T. Binz and S. Swaminathan. Structural analysis of botulinum neurotoxin type E catalytic domain and its mutant Glu212->Gln reveals the pivotal role of the Glu212 carboxylate in the catalytic pathway. *Biochemistry,* 2004, **43**, 6637-6644.

2. S. Jayaraman, S. Eswaramoorthy, D. Kumaran and S. Swaminathan. A common binding site for disialyllactose and a tri-peptide in the C-fragment of tetanus neurotoxin. Proteins, in Press, 2005.

3. Swaminathan has been invited to write a chapter on botulinum structures to be published by CRC (2005).

Conclusions

In our studies we have shown that the ganglioside binding site could be blocked with small molecules and could be used as inhibitor molecules to block botulinum toxicity. We have also shown residues important for the catalytic activity of BoNT/E and the possibility of blocking these residues will inhibit them. Since these residues have the same effect in all serotypes, it may give us some clues for a generic inhibitor for all serotypes.

Plans for the next quarter:

We have identified a peptide by phage display that inhibits BoNT/E activity. We will determine the structure of BoNT/E-LC in complex with that and modify the peptide for better interaction. Virtual screening and x-ray crystallography methods will be combined to identify small molecule inhibitors for BoNT/E. Also structural work on BoNT/B-inhibitor complex will be continued. BBHc will be used to identify molecules to block binding.

Personnel in the Project

1. S. Swaminathan (PI)	Scientist	30% effort
2. S. Eswaramoorthy	Associate Scientist	50% EFFORT
3. R. Agarwal	Research Associate	100% effort

Reference:

1. Swaminathan, S., and Eswaramoorthy, S. (2000) *Nature Struct. Biol.* **7**, 693-699
2. Umland, T. C., Wingert, L. M., Swaminathan, S., Furey, W. F., Schmidt, J. J., and Sax, M. (1997) *Nature Struct. Biol.* **4**, 788-792
3. Navaza, J., and Saludjian, P. (1997) *Methods Enzymol.* **276**, 581-594
4. Jones, T. A., Zou, J., Cowtan, S., and Kjeldgaard, M. (1991) *Acta Crystallogr.* **A47**, 110 - 119
5. Agarwal, R., Eswaramoorthy, S., Kumaran, D., Binz, T., and Swaminathan, S. (2004) *Biochemistry* **43**, 6637-6644
6. Binz, T., Bade, S., Rummel, A., Kollewe, A., and Alves, J. (2002) *Biochemistry* **41**, 1717-1723
7. Rossetto, O., Caccin, P., Rigoni, M., Tonello, F., Bortoletto, N., Stevens, R. C., and Montecucco., C. (2001) *Toxicon* **39**, 115-1159
8. Lister, S. A., Wetmore, D. R., Roche, R. S., and Codding, P. W. (1996) *Acta Crystallogr.* **D52**, 543-550

Appendix 1: Manuscript accepted for publication by Proteins

A common binding site for disialyllactose and a tri-peptide in the C-fragment of tetanus neurotoxin

Seetharaman Jayaraman, Subramaniam Eswaramoorthy, Desigan Kumaran and Subramanyam Swaminathan*

Biology Department, Brookhaven National Laboratory, Upton, New York 11973, USA

*Corresponding Author:

S. Swaminathan

Biology Department

Brookhaven National Laboratory

Upton, NY 11973

Email: swami@bnl.gov

Phone: (631)344-3187

Fax: (631)344-3407

Short title: The receptor binding sites of tetanus toxin

Key Words: Tetanus toxin, GD3, Ganglioside, X-ray crystallography, β-trefoil, Inhibitors

Abstract:

Clostridial neurotoxins comprise of botulinum (BoNT) and tetanus (TeNT) that share significant structural and functional similarity. The crystal structures of the binding domain of TeNT complexed with disialyllactose (DiSia) and a tri-peptide Tyr-Glu-Trp (YEW) have been determined to a resolution of 2.3 and 2.2 Å, respectively. Both DiSia and YEW bind in the shallow cleft region on the surface of the molecule in the β-trefoil domain interacting with a set of common residues Asp1147, Asp1214, Asn1216 and Arg1226. The DiSia and YEW binding at the same site in tetanus toxin provides a putative site that could be occupied either by a ganglioside moiety or a peptide. The soaking experiment of a mixture of YEW and DiSia shows that YEW competes with DiSia and suggests that YEW can be used to block ganglioside binding. A comparison with TeNT binding domain with small molecule complexes and BoNT/A and /B provides insight into the different modes of ganglioside binding.

Introduction:

The clostridial neurotoxins consist of tetanus (TeNT)[1] and botulinum neurotoxins (BoNT) produced by anaerobic bacteria *Clostridium tetani* and *Clostridium botulinum,* respectively, which are the most potent neurotoxins. These toxins follow multi-step mechanisms to exert their biological effects on the target nerve cells[1]. BoNT acts at peripheral nervous system and TeNT acts at the central nervous system. TeNT is the sole

[1] Abbreviations used are: Sia; sialyllactose, DiSia ; disialyllactose, TeNT, tetanus toxin C-fragment, BoNT; botulinum neurotoxin, lac; lactose, NAG; Gal-NAc, ESI-MS; Eletrospray ionization mass spectrometry

causal agent for tetanus which is characterized by generalized rigidity and convulsive spasms of skeletal muscles, while BoNT is responsible for botulism resulting in flaccid paralysis and death[2]. BoNT (seven serotype, A to G) and TeNT share significant sequence homology, and structural and functional similarity. These toxins consist of a single inactive polypeptide chain of 150 kDa that is cleaved by tissue proteinases into an active dichain molecule with a carboxyl-terminal heavy chain of ~100 kDa and an amino terminal light chain of ~50 kDa linked by a disulfide bond. The heavy chain can be further cleaved into two fragments H_N (~50 kDa N-terminal fragment) and H_C (~50 kDa C-terminal fragment) by papain digestion. The H_C fragment plays the primary role in receptor binding[3,4] while the H_N is involved in translocation of the enzymically active light chain through the endosomal membrane into the cytosol[5]. The x-ray crystal structures of the H_C fragment of TeNT[6], BoNT/A[7] and BoNT/B[8] show two domains within H_C, N-terminal and C-terminal domains[6-8]. The N-terminal domain is a jelly-roll motif, closely similar to that of legume lectins which are carbohydrate binding proteins[9]. The C-terminal is a β-trefoil domain[6-8] that is required for cell binding.

Gangliosides consist of oligosaccharide (either linear or branched) group linked to ceramide. The toxin-ganglioside binding is characterized by the amino acid sequence homology among BoNT (A to G) and TeNT which suggests that a conserved amino acid motif of the β-trefoil domain may define a common carbohydrate recognition site. TeNT has been shown to specifically bind gangliosides of the G1b series, GD1b or GT1b[10-12]. To understand the ganglioside-toxin association various experimental strategies like binding[13];Rummel, 2003 #612}, mutagenesis[3,14], photoaffinity[15], x-ray studies[7,8,10,16,17]

and computational docking studies[18,19] have been done. These studies identify binding regions, binding mechanism, affinity and preferred sugar moieties for optimum binding. Binding studies of TeNT with gangliosides show the importance of the presence of disialic acid moiety and also Galβ3GalNAc disaccharide moiety for the tight binding[12,20]. Mutagenesis studies[3] suggest that the C-terminal residues 1306-1310 are essential for cell and ganglioside binding and photoaffinity studies[15] show carboxyl-terminal 34 amino acids of TeNT (residues 1282-1315) are sufficient to support binding of gangliosides that have NeuAcα2,8NeuAc moiety. Recent analysis of mutants of TeNT show His1271-Asp1282 and Asp1214-Asn1219[21] and the region around Tyr 1290[14] provide key residues for ganglioside binding. The x-ray crystal structures of TeNT with lactose, galactose, GalNAc, sialic acid[10] and GT1b analog[17] show the presence of four different sites on the surface of TeNT which are spaced at least 10Å from each other. The results showed that there are two distinct binding sites for GT1b in TeNT. Docking, ESI-MS and NMR studies show that these binding regions can also bind other small molecules and peptides[19] and also find new binding sites that are near the known and putative binding sites. The tri-peptide Tyr-Glu-Trp (YEW) was identified as one of the suitable molecules that bind to a new site that is close to the ganglioside binding site. We are interested in x-ray studies with ganglioside molecules and non-ganglioside molecules like a peptide to explore whether they bind in the existing sites or new sites. As no efficient drug therapy is yet available for tetanus or botulinum, the study to identify suitable inhibitors to block ganglioside binding could lead to structure-based drug design for these toxins.

We have determined the structures of TeNT with DiSialyllactose (DiSia), a ganglioside sugar moiety (GD3), and a tri-peptide Tyr-Glu-Trp (YEW) to gain insights into designing of effective inhibitors with improved specificity and affinity for TeNT. These complexes reveal that both DiSia and YEW bind to TeNT in the same shallow region on the surface of molecule at the β-trefoil domain. A comparison with other TeNT complexes, BoNT/A and B is presented.

Materials and methods

TeNT-DiSia complex:

The recombinant tetanus toxin C fragment, which constitutes the binding portion of the native tetanus toxin, was purchased from Roche Chemicals Co. The lyophilizate is salt-free and contains no protein carrier. The purity of the protein sample was confirmed by gel electrophoresis. The protein was prepared as described in the original paper[22]. The protein was reconstituted with 100 mM $NaHCO_3$ at pH 7.8 to a protein concentration of 10 mg/ml. The solution was dialyzed against 100 mM $NaHCO_3$ at pH 7.8 for 24 hrs in two steps at 4°C. The buffer in the protein solution was then exchanged by dialysis to 10 mM Tris-HCl, pH 7.8 for 24 hours again in two steps. The protein was then concentrated to 8 mg/ml. Crystallization was set up with a droplet containing a mixture of 1 µl protein and 1 µl - 3 µl reservoir solution. The reservoir solution consists of 15% PEG4000, 100 mM imidazole and 50 mM NaCl or $MgCl_2$. Soaking experiments with various concentrations (10 mg/ml to 50 mg/ml) of disialyllactose and duration of soaking ranging from 12 to 48 hrs were carried out and X-ray diffraction data were collected. The

optimum concentration and soaking time were identified as 25mg/ml and 36 hrs, respectively.

Data were collected at liquid nitrogen temperature at X12C beam line of the NSLS, Brookhaven National Laboratory with Brandeis CCD based B4 detector. An oscillation range of 1° was used for each data frame with crystal to detector distance of 100 mm and $\lambda = 1.01$ Å. Data were processed by HKL2000[23](Table I).

The molecular replacement method using AMORE[24] was used to solve the structure of the TeNT-DiSia complex. The crystal structure of the binding domain of TeNT[6] was used as the initial model. After initial rigid body refinement, the structure was refined with CNS[25] and the model was examined with O[26]. The model was complete except that side chains in the 940-948 region were disordered. A sigma-weighted Fo-Fc map was calculated with refined models. The initial map showed clear density for the two sialic acid and Gal residues. The coordinates for Sia and Gal residues were taken from the protein data bank (code: 1F31). The sialic acid and Gal molecules were fitted into the density and refined. Subsequent refinements showed density for the Glc residue. O[26] was used to build the molecule into the electron density.

TeNT-YEW complex:

Crystals of TeNT were soaked with YEW peptide (20 mg/ml) for 48 hrs and data were collected as described above. The data collection and refinement statistics are listed in Table I. Initial maps showed clear density for all three peptide residues except for the

side chain atoms of Glu. The peptide was built in the electron density using O[26] and refined using CNS[25]. Figure 1 shows the schematic diagram of DiSia (αNeu5Ac(2,8)αNeu5Ac(2,3)βDGal(1,4)DGlc) and Figures 2a and 2b show the Sigmaa weighted 2Fo-Fc electron density contoured at 1σ level for DiSia and YEW, respectively.

Results and Discussion:

The structures of TeNT-DiSia and TeNT-YEW complexes were determined at 2.3 and 2.2 Å, respectively. The overall structure of TeNT is well-ordered and has 441 residues from 875 to 1315 and is very similar to that of the native structure[6]. The geometry of the models are reliable with 82% (TeNT-DiSia) and 83% (Tent-YEW) of the residues in the most favored region and the rest in the generously allowed region of the Ramachandran plot as defined by PROCHECK[27].

***TeNT-DiSia complex*:**

The observed binding interactions between DiSia and TeNT are shown in Figure 3a and possible interactions are listed in Table II. The binding site is in the shallow cleft region on the surface of the molecule formed by three loops, Asp1214-Ala1217 on one side, and Asn1144-Asp1147 and Tyr1229-Ala1231 on the other side (Figure 1a, Reference 6). The two Sia residues interact extensively with the enzyme, and Gal and Glc residues are solvent exposed. Sia1 makes direct hydrogen bonds with the side chains of Asn1216, Asp1147 and Arg1226 (Table. II), and Sia2 is stabilized by interactions with Asp1214, Asn1216, Arg1226 and Tyr1229. Recent site-directed mutagenesis experiments showed that the mutation of key residues Asp1214-Asn1219 resulted in substantially reduced

ganglioside binding showing their importance in binding the ganglioside[21]. One of the interactions, the salt bridge observed in TeNT between the guanidino group of Arg1226 and carboxylate oxygens (O1A and O1B) of sialic acid (Sia2) (Table II) is conserved in GT1b and Sia complexes and is characteristic of TeNT-ganglioside recognition[10,28]. Gal3 and Glc4 do not form any hydrogen bonds with the protein. These are more solvent exposed and are stabilized by intra-molecular hydrogen bonds with bound Sia2. O4 of Gal3 forms three intramolecular hydrogen bonds with O6 and O9 of Sia2 and O4 of Glc4. The shortest distance between Glc-O6 and Arg1168 of the symmetry related molecule is 4.9Å.

Though GT1b binds to BoNTs and TeNT, their modes of binding are different. In TeNT there are two sites (Fig. 4) where two independent GT1b molecules bind[29]. One of the sites (Site 1, variantly called lactose binding site of TeNT or sialic acid binding site of BoNT) seems to be common to both. However, the mode of interaction is different. While lactose interacts with the protein in this site of TeNT, sialic acid interacts with the protein in BoNT. This has been confirmed by mutational studies also[30]. BoNT/B binds sialic acid[8] in a cleft (Site 1, Fig. 3) between residues His1240 and Trp1261. In TeNT, lactose interacts with residues in this site. Site 2, called sialic acid binding site of TeNT, though structurally present in BoNT does not bind any part of GT1b in BoNT. This results in only one GT1b molecule binding to BoNT unlike TeNT. The Sia binding site of TeNT is structurally and sequentially very dissimilar to BoNT/B and this brings out the differences of the toxin-ganglioside interactions between BoNT/B and TeNT. Though a moiety of ganglioside binds BoNT/B in Site 1, no structural information is available about the interaction of any other GT1b moiety with the neurotoxin.

Comparison with GT1b complex:

DiSia (GD3 sugar moiety) forms one branch of GT1b oligosaccharide (Neu5Acα(2,3)Galβ(1,3) GalNAcβ(1,4) *(Neu5Acα(2,8)Neu5Acα(2,3))* *Galβ(1,4)Glcβ(1,1)* Ceramide, the DiSia portion of GT1b is italicized and underlined). In GT1b complex Gal and GalNAc residues interact with one TeNT molecule (around residues Tyr1290 and His1271) and the two Sia residues interact with a symmetry related molecule (around residues Asp1147 and Arg1226) and GT1b acts as a cross-linker for the protein. A comparison of GT1b complex with the DiSia complex shows the following three differences. (i) The interactions of Sia7 OA1 (Sia2 in DiSia complex) with Asn1216 OD1 (5.3 Å separated in the DiSia complex) and Sia6 O10 (Sia1 in DiSia complex) with Asn1216 OD1 (4.7 Å separated in the DiSia complex) observed in the GT1b complex are absent in DiSia complex. (ii) The conformation of Sia2 carboxyl group at α2,3 linkage between Sia2 and Gal3 is equatorial in the GT1b complex and axial in the DiSia complex. GT1b used in GT1b complex is a synthetic compound. The difference between synthetic and wild type GT1b is that the Sia6-Gal2 linkage is α in wild type and β in synthetic. This explains the difference. As there is no interaction with the carboxyl group, this conformational change does not affect the binding. The closest distance between OA1 of the carboxyl group of Sia2 and Glu1147 OD2 is 4.8Å in DiSia complex and closest distance between OA1 of the carboxyl group and Lys1143NZ is 6.6Å in the GT1b complex. There is enough space around the carboxyl group of Sia6 for any desired conformation. There are no steric clashes. (iii) Since the α(2,3) linkage between Sia2 and Gal3 is different from its corresponding linkage at GT1b analog the Gal and Glc of DiSia coincide with NGA and Gal (instead of Gal and Glc) of GT1b

analog. Except these three differences the overall binding interactions of Sia1 and Sia2 are similar to the head group of GT1b sugars. These differences suggest that DiSia might represent the true interactions between the GT1b and the protein than the GT1b analog. Though the glycerol group of Sia1 and Sia2 are more flexible, they have the same interactions and conformation in both GT1b and DiSia complex. The interactions of the sialic acid carboxylate and glycerol groups with the protein have been found to be specificity determinants[31] and conserved in the present complex.

Comparison with Sia complex and native structure:

Comparison of TeNT- Sia complex (PDB code 1DFQ) with TeNT-DiSia complex shows that the two Sia residues of DiSia complex bind in the same region with the same set of residues Asp1147, Asp1214, Asn1216 and Arg1226 but the two Sia residues of DiSia complex are positioned on either side of the Sia position of the Sia complex. The interactions between Sia and Asp1214 and Asp1147 are water mediated in Sia complex and the waters are replaced by O4 and O10 of Sia1 and O1A and O1B of Sia2 in DiSia complex. It is interesting to note that TeNT binds a mono or disialic acid in the same region with same set of residues.

A comparison of this complex with the native structure[6] in the binding region shows two minor changes. The first difference is that the side chain of Asn1216 rotates by about 60° in $\chi 2$ to facilitate formation of hydrogen bond with O10 of Sia2. The other difference is that the guanidino group of Arg1226 side chain rotates ~90° in $\chi 4$ to interact with the carboxyl group of Sia2. There are no other significant movements observed in the

binding region. The overall comparison shows that the regions of 940-948 and 1274-1278 are seen to differ considerably between native and this complex. Neither of the regions is close to the binding site nor likely to influence the binding interactions.

TeNT - YEW Complex:

The tri-peptide YEW binds TeNT in the same site as DiSia binding and provides an example of non-ganglioside molecule binding to the ganglioside-binding site. This result shows that this site can bind either sugars or peptides. The difference electron density could unambiguously be interpreted as density representing YEW, though the density for the side chain of Glu was initially absent. The YEW interactions with TeNT are shown in Figure 3b and possible hydrogen bonds are listed in Table III. The observed interactions between tri-peptide and protein residues indicate that the tri-peptide is bound in a fashion similar to that of DiSia. The N-terminal amino group of YEW forms hydrogen bonds with Asn1230 and Ala1231 through water molecules whereas C-terminal Trp side chain fits well the pocket formed by residues Tyr1148, Lys1143, Asp1278 and Asp1147. The middle residue Glu of YEW interacts with Ans1216, Ile1224 and Arg1226. Modeling suggests that even bulkier amino acid residue could be accommodated to improve interactions with the protein. The tri-peptide bound region shows that there is enough room for the peptide to extend on the N-terminal side also. So a tetra or penta peptide can also bind this region. The side chains of YEW form a number of van der Waals contacts with the enzyme to further stabilize the complex.

Comparison of DiSia and YEW complex shows that Asp1147, Asp1214, Asn1216 and Arg1226 are the common residues involved in binding YEW and DiSia in both complexes. The observed interactions in the two complexes are slightly different but comparable and provide a unique stabilizing effect in this region. These residues are involved in Sia and NAG[10] binding also. Asp1214, Asp1147 and Arg1226 play key role in stabilizing any bound receptor in this region. Deletion or mutation of these key residues to Ala or Ser significantly reduces the binding activity of this site[14,21].

As both YEW and DiSia bind in the same site, soaking experiments with a mixture of YEW and DiSia in equimolar concentration was tested and the results showed that YEW competes with DiSia and binds at the site as confirmed by crystal structures (data not shown). This suggests that YEW can be used as an inhibitor to block the binding of ganglioside GT1b at least on one site.

Water molecules play an important role in stabilizing the peptide in the region. Similarly when Sia and NAG[10] bind in this region, water plays an important role. Interestingly, when DiSia bind in the region all water molecules are displaced. The water molecule W2 mimics the DiSia Sia2 carboxylate atoms O1A and OA2 (W2 is 1.1 Å away from both these atoms) and forms similar hydrogen bonds with YEW in the binding site. These water molecules are well buried in the molecule and have low temperature factors, showing their stability. This structure is consistent with earlier ES-MSI study[19].

Comparison of TeNT with BoNT/A and BoNT/B.

The sequence and structure of the β-trefoil domain of TeNT, BoNT/A and B are compared in the different binding sites of TeNT to characterize this site in BoNT/A and B. Figure 5a shows the superposition of the Cα atoms of BoNT/A (red), BoNT/B (blue) with TeNT (green). The alignment is structure based. Though there are sequence alignments in the loop region they are not considered for superposition as the loop orientations differ. The r.m.s. deviation between TeNT and BoNT/A is 0.9 Å and between TeNT and BoNT/B is 0.7 Å for 52 Cα positions. The sequence alignment of TeNT with BoNT/A and B in the β-trefoil region done by CLUSTALW program[32] is shown in Figure 5b.

Site 1: While TeNT binds lactose and part of GT1b (Gal-GalNac), BoNT/B binds Sia and doxorubicin in this region. In BoNT/B, doxorubicin competes with GT1b for binding[18]. This suggests that in BoNT/B, sialyllactose binding site will be that of GT1b. This site is structurally and sequentially well conserved, as they come from conserved secondary structure elements and loops which are structurally similar. This binding site has been predicted by various biochemical studies that indicated β-trefoil subdomain of clostridial neurotoxins was involved in ganglioside binding. Site directed mutagenesis showed that Tyr1290 of TeNT play a key role in binding of ganglioside[14]. This is conserved in BoNT/A (Tyr1266) and BoNT/B (Tyr1262). A study using novel ganglioside photoaffinity ligand implicated that His1293 in TeNT[3] is important in binding. Gln1269 in BoNT/A and Glu1265 in BoNT/B can play the similar role as His1293 in TeNT with a similar stacking of the side chain of Trp1289 which is used to maintain the binding pocket in proper shape for the binding to occur. In addition, it was

shown that ganglioside quenches tryptophan fluorescence, suggesting that Trp1265 must be part of ganglioside binding site in BoNT/A[33]. This is Trp1261 in BoNT/B which contributes to binding of Sia in this region. As BoNT/A has the same sequence and structural motif, it is also expected to bind ganglioside in this region. However, in all these structures this tryptophan provides only stacking interactions. This site is a conserved site and represents the general binding pocket of clostridial neurotoxins. By identifying suitable ligands to this site, they can be used for the entire family of clostridial neurotoxins with increased affinity and specificity.

Though this site is common to both BoNTs and TeNT, the interaction with sugars are different[30]. While Sialic acid interacts with the protein BoNT, lactose interacts in TeNT. Mutation studies have demonstrated that the effect of mutating Tyr1290 (or the corresponding residues in BoNTs) affect the toxicity differently. Tyr 1262 makes two strong hydrogen bonds in BoNT/B while corresponding interactions are absent in TeNT.

Site 2: This site binds Sia, Lac, DiSia (GD3), YEW and Gal-NAc part of GT1b. This region is mainly formed by loops (loop1: residues 1141-1147; loop2: residues1229-1235; loop3: residues 1274-1280). The length and orientation of the loops forming the binding site are different. Loop1 is close to the binding site in TeNT, away by about 7Å in BoNT/B and absent in BoNT/A. This loop is shorter in TeNT (7 residue long) and longer in BoNT/B (10 residue long). Loop2 in BoNT/A and B is oriented about 90° from corresponding TeNT loop. Loop3 is of same length in TeNT, BoNT/A and B but has different orientation. The key residues Asp1214, Asn1216, Asp1147 and Tyr1229 that interact with bound ligands in TeNT are on the loop and are not conserved in BoNT/A

and B, though BoNT/A and BoNT/B show some conservation between them (Glu1202 and Leu1205 in BoNT/A correspond to Glu1188 and Leu1192 in BoNT/B, respectively) (Fig. 5a and 5b). This is a unique binding site for TeNT but differs structurally and sequentially from BoNT/A and B and is probably the reason why this does not act as a binding site for BoNT/A or /B. Bavari et al.[34] have shown that two peptides (corresponding to aa 1157-1181 and aa 1230-1253 of TeNT) induce massive protective immunity against BoNTs. It is interesting to see that the tri-peptide YEW interacts with residues in this region and accordingly YEW may be a part of the antibody. Also, it has been suggested that in double receptor model, this site occupied by ganglioside may later be displaced by the second receptor, a glycoprotein[29] and might provide the necessary protein-protein interaction. A peptide binding in this region also suggests that this may be a common site for sugars and peptides. Since DiSia is GD3 sugar, it is possible that TeNT might bind to GD3 but BoNTs will not.

Conclusion:

The results show that both DiSia and YEW bind in the same region and YEW competes with DiSia and can be used as an inhibitor for the binding site. The DiSia binding characterizes ganglioside binding to TeNT and could be the binding site for GD3, and YEW binding shows that this binding site of TeNT is unique. The comparison study shows that though TeNT has two binding sites, Site 2 a unique binding site for TeNT and Site 1 a common site for all clostridial neurotoxins. The inhibitors to the conserved site remain the most practical target. As TeNT has multiple binding sites, if ligands which simultaneously bind to two adjacent sites can be identified, they can be used to develop bidendate reagents for TeNT and BoNT family.

Acknowledgements

Research supported by the U.S Army Medical Research Acquisition Activity (Award No. DAMD17-02-2-0011) under DOE Prime Contract No. DE-AC02-98CH10886 with Brookhaven National Laboratory. We thank Dr. A. Saxena for providing beam time at the National Synchrotron Light Source, Brookhaven National Laboratory.

References:

1. Schiavo G, Matteoli M, Montecucco C. Neurotoxins affecting neuroexocytosis. Physiol. Rev. 2000;80:717-766.
2. Blasi J, Chapman ER, Yamasaki S, Binz T, Niemann H, Jahn R. Botulinum neurotoxin C blocks neurotransmitter release by means of cleaving HPC-1/syntaxin. EMBO J. 1993;12:4821-4828.
3. Halpern JL, Loftus A. Characterization of the receptor-binding domain of tetanus toxin. Nature 1993;268:11188-11192.
4. Shone CC, Hambleton P, Melling L. Inactivation of Clostridium botulinum type A neurotoxin by trypsin and purification of two tryptic fragments. Proteolytic action near the COOH-terminus of the heavy subunit destroys toxin-binding activity. Eur. J. Biochem. 1985;151:75-82.
5. Shone CC, Hambleton P, Melling J. A 50-kDa fragment from the NH2-terminus of the heavy subunit of Clostridium botulinum type A neurotoxin forms channels in lipid vesicles. Eur. J. Biochem. 1987;167:175-180.
6. Umland TC, Wingert LM, Swaminathan S, Furey WF, Schmidt JJ, Sax M. Structure of the receptor binding fragment H_c of tetanus neurotoxin. Nature Struct. Biol. 1997;4:788-792.
7. Lacy DB, Tepp W, Cohen AC, DasGupta BR, Stevens RC. Crystal structure of botulinum neurotoxin type A and implications for toxicity. Nat. Struct. Biol. 1998;5:898-902.

8. Swaminathan S, Eswaramoorthy S. Structural analysis of the catalytic and binding sites of *Clostridium botulinum* neurotoxin B. Nat. Struct. Biol. 2000;7:693-699.

9. Pellizzari R, Rossetto O, Schiavo G, Montecucco C. Tetanus and botulinum neurotoxins: mechanism of action and therapeutic uses. Philos. Trans. R. Soc. Lond. B. Biol. Sci. 1999;354:259-268.

10. Emsley P, Fotinou C, Black I, Fairweather NF, Charles IG, Watts C, Hewitt E, Isaacs NW. The structures of the H(C) fragment of tetanus toxin with carbohydrate subunit complexes provide insight into ganglioside binding. J. Biol. Chem. 2000;275:8889-8894.

11. Rogers TB, Snyder SH. High affinity binding of tetanus toxin to mammalian brain membranes. J. Biol. Chem. 1981;256:2402-7.

12. Holmgren J, Elwing H, Fredman P, Svennerholm L. Polystyrene-adsorbed gangliosides for investigation of the structure of the tetanus-toxin receptor. Eur. J. Biochem. 1980;106:371-9.

13. Louch HA, Buczko ES, Woody MA, Venable RM, Vann WF. Identification of a binding site for ganglioside on the receptor binding domain of tetanus toxin. Biochemistry. 2002;41:13644-52.

14. Sutton JM, Chow-Worn O, Spaven L, Silman NJ, Hallis B, Shone CC. Tyrosine-1290 of tetanus neurotoxin plays a key role in its binding to gangliosides and functional binding to neurones. FEBS Lett. 2001;493:45-9.

15. Shapiro RS, Specht CD, Collins BE, Woods AS, Cotter RJ, Schnaar RL. Identification of a ganglioside recognition domain of tetanus toxin using a novel ganglioside photoaffinity ligand. J. Biol. Chem. 1997;272:30380-30386.

16. Eswaramoorthy S, Kumaran D, Swaminathan S. Crystallographic evidence for doxorubicin binding to the receptor-binding site in *Clostridium botulinum* neurotoxin B. Acta Cryst. 2001;D57:1743-1746.

17. Fotinou C, Emsley P, Black I, Ando H, Ishida H, Kiso M, Sinha KA, Fairweather NF, Isaacs NW. The crystal structure of tetanus toxin Hc fragment complexed with a synthetic Gt1b analogue suggests cross-linking between ganglioside receptors and the toxin. J. Biol. Chem. 2001;276:32274-32281.

18. Lightstone FC, Prieto MC, Singh AK, Piqueras MC, Whittal RM, Knapp MS, Balhorn R, Roe DC. Identification of novel small molecule ligands that bind to tetanus toxin. Chem. Res. Toxicol. 2000;13:356-362.

19. Cosman M, Lightstone FC, Krishnan VV, Zeller L, Prieto MC, Roe DC, Balhorn R. Identification of novel small molecules that bind to two different sites on the surface of tetanus toxin C fragment. Chem. Res. Toxicol. 2002;15:1218-28.

20. Angstrom J, Teneberg S, Karlsson KA. Delineation and comparison of ganglioside-binding epitopes for the toxins of Vibrio cholerae, Escherichia coli, and Clostridium tetani: evidence for overlapping epitopes. Proc. Natl. Acad. Sci. USA. 1994;91:11859-63.

21. Sinha K, Box M, Lalli G, Schiavo G, Schneider H, Groves M, Siligardi G, Fairweather N. Analysis of mutants of tetanus toxin Hc fragment: ganglioside binding, cell binding and retrograde axonal transport properties. Mol. Microbiol. 2000;37:1041-51.

22. Umland TC, Wingert L, Swaminathan S, Schmidt JJ, Sax M. Crystallization and preliminary X-ray analysis of tetanus neurotoxin C fragment. Acta Crystallographica 1998;D54:273-275.

23. Otwinowski Z, Minor W. Processing of X-ray diffraction data collected in oscillation mode. Methods Enzymol. 1997;276:307-326.

24. Navaza J, Saludjian P. AMoRe: An automated molecular replacement program package. Methods Enzymol. 1997;276:581-594.

25. Brunger AT, Adams PD, Clore GM, Delano WL, Gros P, Grosse-Kunstleve RW, Jiang JS, Kuszwewski J, Nilges M, Pannu NS and others. Crystallography & NMR system: a new software suite for macromolecular structure determination. Acta Crystallogr. 1998;D54:905-921.

26. Jones TA, Zou J, Cowtan S, Kjeldgaard M. Improved methods in building protein models in electron density map and the location of errors in these models. Acta Crystallogr. 1991;A47:110 - 119.

27. Laskowski RA, MacArthur MW, Moss DS, Thornton JM. PROCHECK: a program to check the stereochemical quality for assessing the accuracy of protein structures. J. Appl. Crystallogr. 1993;26:283-291.

28. Fotinou C, Emsley P, Black I, Ando H, Ishida H, Kiso M, Sinha KA, Fairweather NF, Isaacs NW. The crystal structure of tetanus toxin Hc fragment complexed with a synthetic GT1b analogue suggests cross-linking between ganglioside receptors and the toxin. J Biol Chem. 2001;276:32274-81.

29. Rummel A, Bade S, Alves J, Bigalke H, Binz T. Two carbohydrate binding sites in the H(CC)-domain of tetanus neurotoxin are required for toxicity. J. Mol. Biol. 2003;326:835-847.

30. Rummel A, Mahrhold S, Bigalke H, Binz T. The HCC-domain of botulinum neurotoxins A and B exhibits a singular ganglioside binding site displaying serotype specific carbohydrate interaction. Mol. Microbiol. 2004;51:631-43.

31. Rini JM. X-ray crystal structures of animal lectins. Curr Opin Struct Biol. 1995;5:617-21.

32. Thompson JD, Higgins DG, Gibson TJ. CLUSTAL W: improving the sensitivity of progressive multiple sequence alignment through sequence weighting, position-specific gap penalties and weight matrix choice. Nucleic Acids Res. 1994;22:4673-4680.

33. Kamata Y, Yoshimoto M, Kozaki S. Interaction between botulinum neurotoxin type A and ganglioside: ganglioside inactivates the neurotoxin and quenches its tryptophan fluorescence. Toxicon 1997;35:1337-1340.

34. Bavari S, Pless DD, Torres ER, Lebeda FJ, Olson MA. Identifying the principal protective antigenic determinants of type A botulinum neurotoxin. Vaccine 1998;16:1850-6.

Figure legends:

Figure 1. Schematic representation of disialyllactose (Di-(N-acetylneuramin)lactose αNeu5Ac(2,8)αNeu5Ac(2,3)βDGal(1,4)DGlc)

Figure 2. Stereodiagram of the sigmaa weighted (2Fo-Fc) electron density maps for (a) disialyllactose and (b) YEW. The maps were computed using the final model and contoured at 1σ level.

Figure 3. Residues of TeNT interacting with (a) disialyllactose and (b) YEW. Bonds and carbon atoms for disialyllactose and YEW are in green while they are in yellow for protein residues. Oxygen and nitrogen atoms are colored red and blue, respectively. Potential hydrogen bonds are shown as dotted lines.

Figure 4. β-trefoil domain of TeNT showing the two binding sites. Trp1289 and Try1290 in site-1 and Asp1147 and Arg1226 in site-2 are labeled.

Figure 5: (a) Stereo view of superposition of BoNT/A (red) and BoNT/B (green) on TeNT. Cα trace is (blue). A key residue (Tyr1290 in Site 1 and Asp1147 in Site 2) in each binding site is shown in ball and stick model. (b). Sequence alignment of TeNT with BoNT/A and B. Site 1 and Site 2 residues are highlighted in yellow and blue, respectively.

Table I. Data reduction and refinement statistics

	TeNT-DiSia	**TeNT-YEW**
Space group	$P2_12_12_1$	$P2_12_12_1$
Molecules per asymmetric unit	1	1
Unit Cell (Å)	a = 70.91 b = 78.93 c = 90.98	a = 67.10 b = 79.20 c = 90.23
Resolution (Å)	2.3	2.2
No. of Unique reflections	23445	25062
Completeness (overall/outershell)	97/81	98/83
R_{merge}	0.053	0.120
R-factor	0.23	0.22
R_{free}	0.28	0.27
No. of protein atoms	3564	3564
No. of water molecules	203	211
No. of heterogen atoms	66	63
Average B factor (Å) Protein Water molecules Heterogens	 39.1 40.3 58.0	 19.8 31.0 32.5

RMSD		
Bond lengths (Å)	0.01	0.01
Bond angles (°)	1.50	1.30

Table II. Disialyllactose TeNT interactions:

Atom1	Atom2	Distance (Å)
Sia1		
O4	Asp1147 OD2	2.5
O4	Asp1147 OD1	3.2
N5	Asp1147 OD1	3.1
N5	Arg1226 NH2	3.2
O10	Asn1216 ND2	2.8
Sia2		
O1B	Arg1226 NH2	2.7
O1A	Arg1226 NH2	3.3
O1A	Agr1226 NH1	3.2
O1A	Asn1216 NH	2.6
O4	Asp1214 O	2.6
O8	Tyr1229 OH	2.5

Table III. TeNT-YEW Interaction:

Atom1	Atom2	Distance (Å)
YEW Trp NE1	1147 Asp OD1	2.9
1226 Arg NH2	Wat1	2.6
Wat1	YEW Glu O	2.5
Wat1	Asn1216 N	2.9
YEW Glu N	Wat1	2.8
YEW Glu OE1	1214 Asp O	2.9
1130 Asn N	Wat2	2.7
Wat2	Wat3	2.9
Wat3	YEW Tyr OH	2.9
1231 Ala N	Wat3	3.2
YEW Tyr O	Wat4	2.8
Wat4	1213 Lys O	2.9

Fig. 1

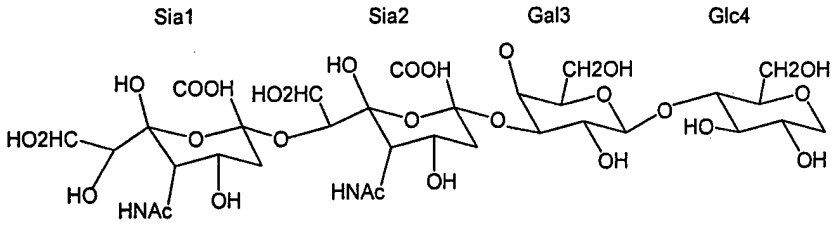
Sia1
Sia2
Gal3
Glc4
HO
COOH
HO2HC
HO2HC
HO
HO
HNAc
OH
HO
COOH
HNAc
OH
O
CH2OH
OH
CH2OH
HO
OH
O

Figure 2a and 2b.

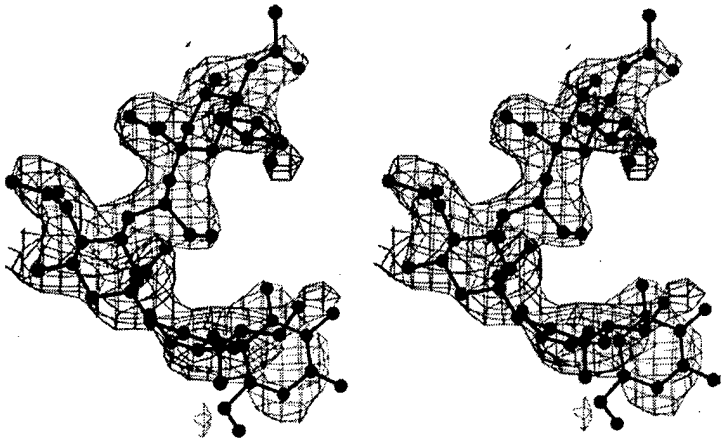

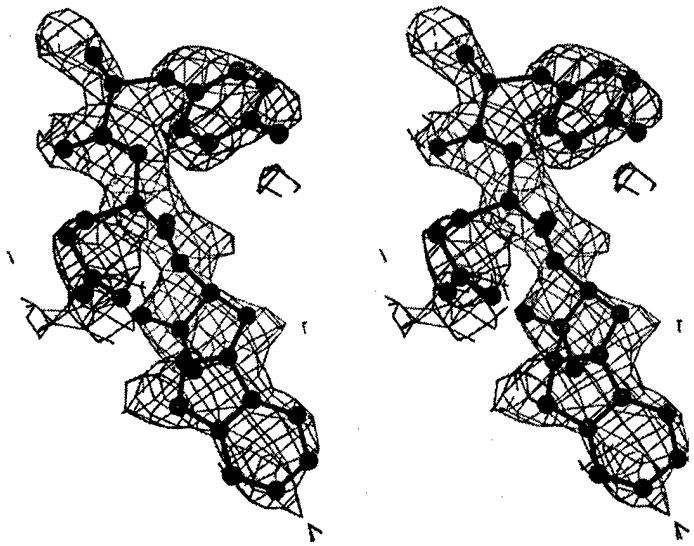

Figures 3a and 3b

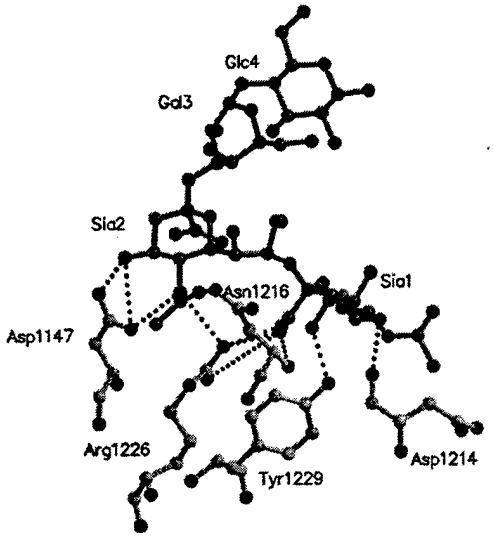

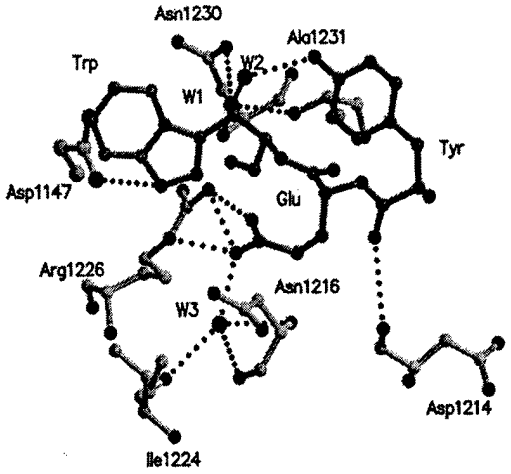

Figure.4.

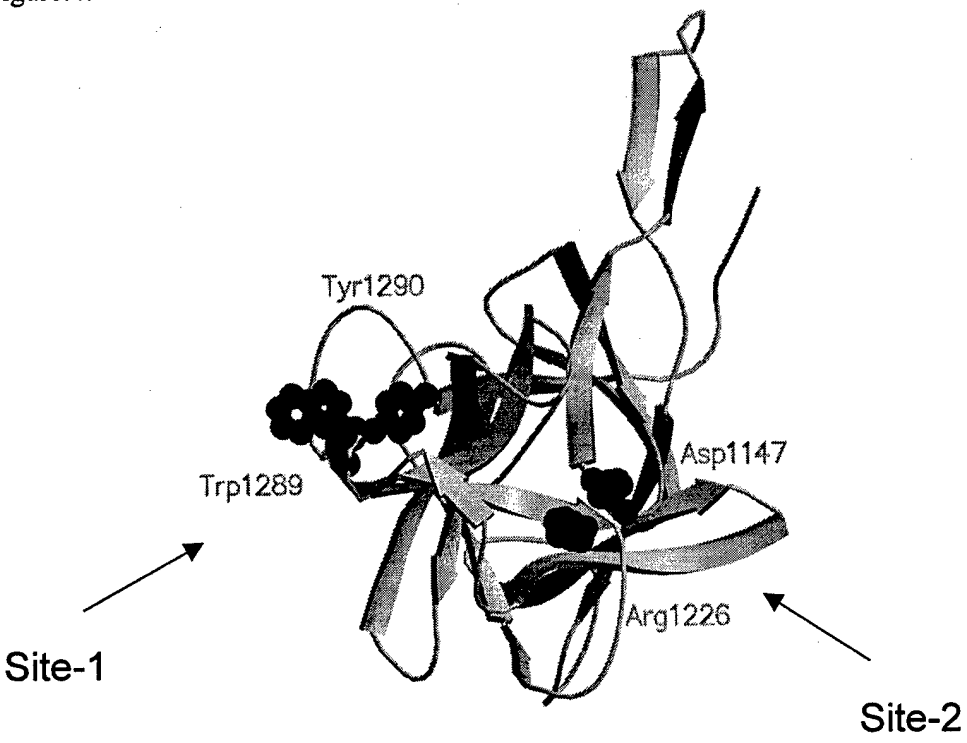

Figure. 5a and 5b.

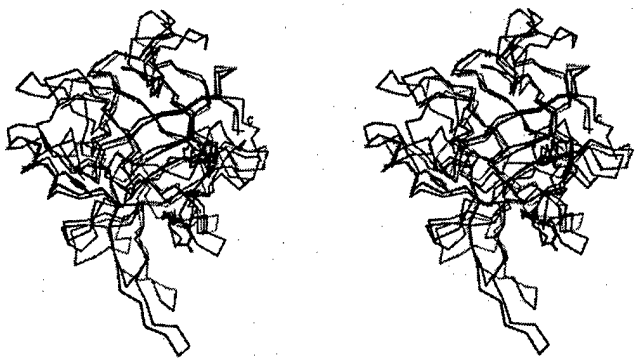

```
TeNT  LRDFWGNPLRYDTEYYLIPVASSSKDVQLKN--ITDYMYLTNAPSYTNGKLNIYYRR-LY 1170
BoTA  LKDFWGDYLQYDKPYYMLNLYDPNKYVDVNNVGIRGYMYLK-GPRGSVMTTNIYLNSSLY 1154
BoTB  --------LMYNKEYYMFNAGNKNSYIKLKKDSPVGEILTR--SKYNQNSKYINYRD-LY 1139

TeNT  NGLKFIIKR-YTPNNEIDSFVKSGDFIKLYVSYNNNEHIVGYPKDGNAFNNLDRILRVGY 1229
BoTA  RGTKFIIKK-YASGN-KDNIVRNNDRVYINVVVKNKEYRLATNASQAGVEKILSALEIPD 1211
BoTB  IGEKFIIRRKSNSQSINDDIVRKEDYIYLDFFNLNQEWRVYTYKYFKKEEEKLFLAPIS- 1198

TeNT  DAPGIPLYKKMEAVKLRDLKTYSVQLKLYDDKNASLGLVGTHNGQIG---NDPNRDILIA 1286
BoTA  DVGNLSQVVVMKSKNDQGITN-KCKMNLQDNNGNDIGFIGFH---------QFNNIAKLVA 1262
BoTB  DSDEFYNTIQIKEYDEQPTYSCQLLFKKDEESTDEIGLIGIHRFYESGIVFEEYKDYFCI 1258

TeNT  SNWYFNHLK----DKILGCDWYFVPTDEGWTND-- 1315
BoTA  SNWYNRQIERS--SRTLGCSWEFIPVDDGWGERPL 1295
BoTB  SKWYLKEVKRKPYNLKLGCNWQFIPKDEGWTE--- 1290
```

Structural Analysis of Botulinum Neurotoxin Type E Catalytic Domain and Its Mutant Glu212→Gln Reveals the Pivotal Role of the Glu212 Carboxylate in the Catalytic Pathway[†,‡]

Rakhi Agarwal,[#] Subramaniam Eswaramoorthy,[#] Desigan Kumaran,[#] Thomas Binz,[§] and Subramanyam Swaminathan*[,#]

Biology Department, Brookhaven National Laboratory, Upton, New York 11973, and Department of Biochemistry, Medizinische Hochschule Hannover, Hannover, Germany

Received December 18, 2003; Revised Manuscript Received March 9, 2004

ABSTRACT: The seven serotypes of botulinum neurotoxins (A−G) produced by *Clostridium botulinum* share significant sequence homology and structural similarity. The functions of their individual domains and the modes of action are also similar. However, the substrate specificity and the peptide bond cleavage selectivity of their catalytic domains are different. The reason for this unique specificity of botulinum neurotoxins is still baffling. If an inhibitor leading to a therapeutic drug common to all serotypes is to be developed, it is essential to understand the differences in their three-dimensional structures that empower them with this unique characteristic. Accordingly, high-resolution structures of all serotypes are required, and toward achieving this goal the crystal structure of the catalytic domain of *C. botulinum* neurotoxin type E has been determined to 2.1 Å resolution. The crystal structure of the inactive mutant Glu212→Gln of this protein has also been determined. While the overall conformation is unaltered in the active site, the position of the nucleophilic water changes in the mutant, thereby causing it to lose its ability to activate the catalytic reaction. The structure explains the importance of the nucleophilic water and the charge on Glu212. The structural differences responsible for the loss of activity of the mutant provide a common model for the catalytic pathway of *Clostridium* neurotoxins since Glu212 is conserved and has a similar role in all serotypes. This or a more nonconservative mutant (e.g., Glu212→Ala) could provide a novel, genetically modified protein vaccine for botulinum.

Clostridium botulinum secretes seven serotypes of botulinum neurotoxins (BoNT,[1] A−G) that are produced as single inactive polypeptide chains of 150 kDa and cleaved into active dichains of heavy (HC, 100 kDa) and light (LC, 50 kDa) chains, linked by a disulfide bond, by endogenous or exogenous proteases. The HC mediates binding to nerve cells and translocation of the catalytical LC into the cytosol following receptor-mediated endocytosis.

Although they all share sequence and possibly structural similarity, each BoNT has exclusive substrate specificity and scissile bond selectivity (*1*). BoNT/A, /C, and /E cleave the synaptosomal-associated 25-kDa protein (SNAP-25) at different peptide bonds (*2*−*4*), while BoNT/B, /D, /F, and /G cleave the vesicle-associated membrane protein (VAMP), also known as synaptobrevin (*5*), but again each cuts at a different peptide bond. BoNT/C may be unique since it cleaves both SNAP-25 and syntaxin (*1*). The BoNTs are typical zinc metalloproteases which have a unique conserved zinc binding motif (HExxH + E) in the catalytic domain. The Zn coordinated by two histidines, a glutamate and a water molecule, plays an important role in the catalytic activity.

Even though experimental vaccines are available, no therapeutic treatments are on hand to date. To develop a successful vaccine/inhibitor/antitoxin for the toxins, an understanding of the molecular mechanism, especially catalysis by catalytic domain, is a prerequisite. This will help in rational structure-based drug design in the treatment of botulism.

A large body of information on chemical, biological, and pathological aspects of *Clostridium* neurotoxins is available now, but structural information for the holotoxin is available only for BoNT/A at 3.3 Å (*6*) and BoNT/B at 1.8 Å (*7*). Three-dimensional structures are also available for BoNT/A-LC (unpublished work), BoNT/B-LC (*8*), and the C-fragment of tetanus toxin (*9*, *10*). But this is the first structural report for any of the domains of BoNT/E. The crystal structures of BoNT/E-LC and its mutant Glu212Gln are reported here. Comparison of the structures of BoNT/A, BoNT/B, and BoNT/E LCs would provide a basis for

[†] This research has been supported by the U.S. Army Medical Research Acquisition Activity (Award No. DAMD17-02-2-0011) under DOE Prime Contract No. DE-AC02-98CH10886 with Brookhaven National Laboratory.

[‡] The coordinates for the wild-type (1T3A) and mutant (1T3C) structures are deposited with the Protein Data Bank.

* To whom correspondence should be addressed. E-mail: swami@bnl.gov. Telephone: (631) 344-3187. Fax: (631) 344-3407.

[#] Brookhaven National Laboratory.

[§] Medizinische Hochschule Hannover.

[1] Abbreviations used: BoNT, botulinum neurotoxin; HC, heavy chain; LC, light chain; VAMP, vesicle-associated membrane protein; SNAP-25, synaptosomal-associated 25-kDa protein; DTT, dithiothreitol; HEPES, (*N*-[2-hydroxyethyl]piperazine-*N*′-[2-ethanesulfonic acid]); SAD, single-wavelength anomalous dispersion; GST, glutathione-*S*-transferase.

10.1021/bi036278w CCC: $27.50
Published on Web 05/08/2004

understanding the differences in their specificity and selectivity and information for designing a common inhibitor for all three or any of the serotypes. The difference in structure and function of wild-type and mutant (Glu212Gln) of BoNT/E presents a model for the catalytic pathway of the toxin.

EXPERIMENTAL PROCEDURES

Plasmid Construction, Site-Directed Mutagenesis, and Expression and Purification of BoNT/E-LC Protein. The pET-9c vector encoding the full length of BoNT/E-LC has been constructed as described earlier (*11*). This construct (LC-pET9c) has been expressed in BL21 (DE3) cells, and a high level of expression (>30 mg/L of culture) has been achieved. A full description of expression and purification procedures is given by Agarwal et al. (*11*).

The 46mer complementary PCR primers (Invitrogen) were designed to abolish a restriction site by a silent mutation near the site of target mis-sense mutation. The restriction site for *Nsi*I was abolished (A'TGCAT) with the aim to achieve an easy and fast identification of the probable clones containing the mutation. The mutation site was in the middle region of the primers: forward primer 5'CCT GCT CTT ACA TTA *ATG CAC* CAA TTA ATA CAT TCA TTA CAT GGA C 3' and reverse primer 5'GTC CAT GTA ATG AAT GTA TTA ATT *GGT GCA TTA* ATG TAA GAG CAG G 3'. The underlined 21st and 22nd bases of the forward primer from the 5' end represent the silent mutation (T→C) to abolish the site for *Nsi*I restriction enzyme and the site of mutation GAA → CAA (E→Q), respectively. The corresponding base changes were also made in the complementary reverse primer. The Quick-Change site-directed mutagenesis kit (Stratagene, La Jolla, CA) was used for the mutagenesis according to the manufacturer's manual. Mutated plasmids were identified by performing *Nsi*I restriction digest through the loss of one *Nsi*I cleavage site. The entire region encoding the mutated LC was sequenced in both strands by Big Dye terminator cycle sequencing (Applied Biosystems) and showed the expected mutation.

The plasmid DNA was transfected into *Escherichia coli* BL21 (DE3) bacteria for the expression of the protein. The growth conditions of the culture for expression and purification of protein used were identical to those described for the wild-type protein (*11*). A similar very high-level expression of protein has been obtained (>15 mg/500 mL of culture). This protein was also found to be very stable and soluble.

Enzymatic Activity of Wild-Type and Mutant Proteins. The proteolytic activity of wild-type and mutant BoNT/E-LC has been assayed in vitro on its substrate SNAP-25(1−206aa). The SNAP-25 had an N-terminal GST tag. The assay was performed in a final volume of 20 μL [20 mM HEPES, pH 7.4, 2 mM DTT, 10 μM $Zn(CH_3COO)_2$] containing a 5 nM concentration of LC and a 5 μM concentration of SNAP-25. However, the mutant protein concentration in reaction mixture was varied from 5 to 50 nM. Cleavage of GST-SNAP-25 by the LC was determined by incubating the samples at 37 °C for 60 min. The reactions were stopped by adding 10 μL of 3× concentrated SDS−PAGE sample buffer which contained sufficient EDTA to chelate the Zn cofactor. The extent of cleavage was then evaluated following electrophoresis on 4−20% Tris−glycine SDS−PAGE gels by the appearance and intensity of a new band at ~47 kDa due to the cleavage of the GST-SNAP-25 between aa180 and 181.

Crystallization and Data Collection. The crystallization screening was carried out by the sitting drop vapor diffusion method using Hampton Research crystallization screens as described previously (*11*). Crystals of both wild-type and mutant proteins were obtained under several conditions using ammonium sulfate and/or PEG at various pH values, ranging from 4.6 to 8.5, at room temperature. Diffraction-quality crystals were obtained at room temperature for both wild-type and mutant proteins using 0.5 M ammonium sulfate, 1.0 M Li_2SO_4, and 0.1 M sodium citrate trihydrate at pH 5.6 as precipitant, and crystals grew to their full size in 2−6 days. Crystals belong to the space group $P2_12_12$, with cell dimensions $a = 88.33$, $b = 144.45$, and $c = 83.37$ Å. The Matthews coefficient was calculated to be 2.67 Da/Å^3, assuming two molecules per asymmetric unit. A self-rotation function calculation with MolRep confirmed the presence of a noncrystallographic two-fold axis relating the two molecules in the asymmetric unit (*11*, *12*). The cell parameters for crystals of mutant and wild-type LC are similar.

Since the protein contains one zinc ion per molecule, single-wavelength anomalous dispersion (SAD) data were collected from the crystal of wild-type LC at the zinc absorption edge ($\lambda = 1.2837$ Å) corresponding to the peak obtained at the NSLS beamline X12C with a Brandeis CCD-based B4 detector. The crystal was briefly transferred to the mother liquor containing 15−20% glycerol and was mounted on a nylon loop and flash frozen immediately by plunging into liquid nitrogen. Data covering a total of 360° rotation in ϕ were collected, for an oscillation range of 1° per frame, using the "inverse geometry" method. Crystals diffracted to better than 2.1 Å resolution. Data from mutant crystals were collected at $\lambda = 1$ Å, and the diffraction limit was 1.9 Å. Data were processed with DENZO and scaled and merged with SCALEPACK (*13*). Details of data collection statistics are given in Table 1.

Structure Determination. Initial attempts to determine the structure by the molecular replacement method using BoNT/A or BoNT/B LC as the search model failed. However, the method was not tried extensively. The data collected at the zinc absorption edge were used to solve the structure by the SAD method. The positions of the two zinc atoms were determined from the anomalous difference Patterson maps (*14*). The data were phased using SHARP (*15*) and further improved by noncrystallographic symmetry averaging and solvent flattening using DM (*16*). ARP/wARP (*17*) was used to build the model. About 70% of the model was built automatically by the program, and the rest was built-in manually using "O". The model was refined using CNS (*18*), and the solvent molecules were added using CNS. Initial refinements were carried out using strict NCS restraint. In the final stages this was relaxed, and both monomers were refined as independent molecules. The final model is complete, except for residues 234−244 and the 10 C-terminal residues in both molecules because of weak electron density, indicating that the region may be disordered. The rmsd between the C-α atoms of the two monomers in the asymmetric unit is 0.53 Å, excluding 16 C-terminal residues present in the structure. The two molecules differ in the

Table 1: Crystal Data and Refinement Statistics

	Cell Parameters
wild-type LC	space group $P2_12_12$
	$a = 88.33$, $b = 144.45$, and $c = 83.27$ Å
Glu212Gln-LC	space group $P2_12_12$
	$a = 88.21$, $b = 144.30$, and $c = 82.59$ Å

Phasing Statistics (Wild-Type-LC)

method	SAD
wavelength (Å)	1.2837
anomalous scatterer	zinc
resolution (Å)	2.16
no. of reflections	56 133
overall FOM	0.15
after solvent flattening	0.91

Refinement Statistics

	wild-type LC	Glu212Gln-LC
resolution range (Å)	2.16	1.9
no. of reflections	55 960	74 652
completeness (%)	97.4	89.2
R-factor	0.22	0.24
R-free	0.26	0.29
no. of protein atoms	6315	6562
no. of heterogen atoms	3	4
no. of water molecules	348	493
rms deviations		
bond lengths (Å)	0.006	0.006
bond angles (°)	1.31	1.26

conformation of these C-terminal residues. The final *R* and *R*-free values are 0.22 and 0.26, respectively. A difference Fourier map brought out a chlorine ion near Arg 401. The reliability of the model was checked with PROCHECK (*19*), which showed that 88% of the residues are in the most favored region of the Ramachandran plot.

The structure of the mutant Glu212Gln was determined by the molecular replacement method, and the model was adjusted against a composite omit map to remove the model bias. Initially, during the molecular replacement Glu212 was substituted with alanine and the active-site zinc was not included in the search model. Gln was fitted into the density during model adjustment, and there was clear electron density for zinc. The model was refined using CNS. The final *R* and *R*-free values are 0.24 and 0.29, respectively. Clear electron density for residues 234−244 of the loop region missing in the wild-type protein structure was present in the mutant structure. The refinement statistics are presented in Table 1.

RESULTS AND DISCUSSIONS

Enzymatic Activity of BoNT/E-LC and Its Mutant Glu212Gln. The proteins were overexpressed in BL21 (DE3) cells, and use of the modified protocol as described in the methods section led to a very high recovery of protein. The protein was soluble and maintained its full length only when preserved at <−20 °C. The protein has been found to be temperature sensitive, and the preservation of protein at temperatures 4 °C or above led to the cleavage of ~2 kDa from the N-terminal of the protein.

The 49.7-kDa SNAP-25 tagged with GST (GST-SNAP-25) was used to assay the enzymatic activity of the BoNT/E-LC and its mutant (Glu212Gln). The GST tag was not removed from SNAP-25 since its presence in the fusion protein GST-SNAP-25 does not interfere with the catalytic activity of botulinum neurotoxins (*11*, *20*, *21*).

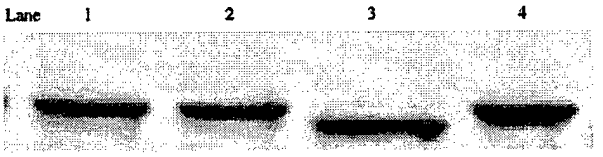

FIGURE 1: Analysis of catalytic activity of Glu212Gln mutant vs wild-type enzyme on its substrate SNAP-25. The reaction samples were run on 4−20% Tris−glycine gel and then stained with Coomassie blue. Lane 1 and 2, 5 and 50 nM mutant with 5 μM SNAP-25; lane 3, 5 nM wild-type enzyme with 5 μM SNAP-25; lane 4, 5 μM SNAP-25 alone. Using higher concentrations of mutant did not result in substrate cleavage.

Incubation of GST-SNAP-25 with BoNT/E-LC resulted in cleavage of peptide bond 180−181 of SNAP-25 and produced two fragments of sizes ~46.8 and ~2.9 kDa. The percentage cleavage of the substrate by enzyme at different time intervals showed that 5 nM LC was able to completely cleave 5 μM SNAP-25 in 15 min of incubation at 37 °C, suggesting that the protein is highly catalytic.

However, the Glu212Gln-LC mutant did not show any detectable activity. Increasing the mutant LC concentration did not lead to any cleavage product visible in the gel (Figure 1). The loss of activity may be because of loss of zinc, since the apo protein devoid of zinc is inactive. Spectroscopic analysis of zinc content was not done in this study and was not necessary, since during X-ray data collection the crystal was scanned at the absorption edge of zinc and a good signal for zinc was obtained, confirming the presence of zinc. Also, the structure determination brought out electron density for zinc.

The loss of catalytic activity could be either due to the enzyme not binding to the substrate or due to the loss of hydrolysis of the peptide. A control experiment was performed to identify the exact reason. The mutant and the substrate were mixed in a 1:1 ratio in the same buffer used for the wild-type enzyme and incubated for 30 min. The wild-type protein was then added in a 1:500 (enzyme to substrate) ratio and incubated at 37 °C for 30 min. An SDS gel was run to compare the results. There was no detectable cleavage of the substrate by the wild-type enzyme when the substrate was premixed with the mutant, indicating that the mutant effectively binds to the substrate and the wild-type enzyme has to compete for the binding site. As another control, the same experiment was repeated with the substrate premixed with an unrelated protein BSA, and the cleaved product was visible in the gel, showing that the binding of mutant to the substrate is specific. The control experiment was also repeated with another unrelated protein lysozyme, giving the same result. These two experiments confirmed that the mutant binds and positions itself for the catalytic activity but the peptide hydrolysis is blocked. In another experiment, we have also found that the Glu212Ala mutant of BoNT/E-LC forms a stable complex with GST-SNAP-25 at 4 °C (unpublished results).

Description of Structures of BoNT/E-LC. (a) Wild-Type BoNT/E-LC. This is the first time, at least to our knowledge, that the crystal structure of a molecule of this size (421 amino acids) has been determined using the anomalous signal from a single zinc atom, even though the contribution to the intensity from the anomalous signal from zinc ($f' = -8.1$

FIGURE 2: Ribbons representation of the dimer of BoNT/E-LC. Thesis composed of one monomer of wild-type (green) and one monomer of mutant (blue). The active-site zinc and coordinating residues are shown in the ball-and-stick model. The dimer is formed by a noncrystallographic two-fold axis passing through the midpoint normal to the plane of the figure. The C-terminal helix in the second monomer is not well ordered.

and $f''= 3.89$) is calculated to be less than 2% at 2.0 Å resolution. Since no other information was used in the structure determination, this must be considered a de novo structure determination without any model bias. Even though crystal structures of BoNT/A-LC and BoNT/B-LC have been determined, both of them are truncated version of the LC, unlike BoNT/E-LC. However, 10 C-terminal residues were not located in the electron density map. But a mass spectroscopic analysis of the protein gave the mass corresponding to full-length LC. Moreover, a few more residues (though disordered) were seen in the mutant structure, confirming that the missing residues are not due to any proteolysis. The BoNT/E-LC forms a dimer in the crystal and presumably a dimer in solution state also (Figure 2). Interestingly, unlike BoNT/A-LC, where the dimer is formed with the active site covered by the dimeric interface (unpublished work), here the active sites are not in the dimeric interface and are exposed to the solvent region. The advantage of this crystal structure is that it can be used for inhibitor studies by soaking native crystals in an inhibitor containing the mother liquor. The dimer is formed by a noncrystallographic two-fold symmetry. The buried surface area at the dimeric interface is 2340 Å^2.

The conformation of BoNT/E-LC is similar to those of BoNT/A-LC and BoNT/B-LC. One major difference may be at the C-terminus (Figure 3a). In BoNT/E-LC, which is a full-length LC, the C-terminal region takes a helical conformation. This region is just before the interchain disulfide bond. In BoNT/A and BoNT/B holotoxin structures, these are β strands. If BoNT/E holotoxin has a similar conformation, the change in conformation may be due to the separation of LC from HC or an artifact of recombinant protein. Since both BoNT/A and /B LCs are truncated LCs, their conformation in this region could not be directly compared with that of BoNT/E-LC.

The active site is similar to other botulinum neurotoxins. The active-site zinc is coordinated by His 211 NE2, His 215 NE2, Glu 250 OE1, Glu 250 OE2, and a nucleophilic water molecule (Figure 4a). The coordinating distances are given in Table 2. The nucleophilic water makes a hydrogen bond of 2.86 Å with Glu 212 OE2. This interaction seems to be important for the activation of the nucleophilic water.

About 45 residues are observed within a sphere of radius 10.0 Å centered on the zinc atom. Comparison of the residues in similar spheres in BoNT/B-LC and BoNT/A-LC brings out some interesting features. A few interactions are common to all of them. Glu 335 makes hydrogen-bonding contacts with Arg 347 and His 211, while Glu 249 interacts with His 215 and His 218, stabilizing the structure and the electrostatic forces (Figure 4). These interactions stabilize the side-chain conformations of His 211 and His 215, allowing them to be properly oriented for zinc coordination. Since these residues are conserved in all *Clostridium* neurotoxins (Figure 5), their role may be the same in all of them. Arg 347 and Tyr 350, which are in the active-site region, are similarly placed in BoNT/B-LC and BoNT/E-LC with respect to the nucleophilic

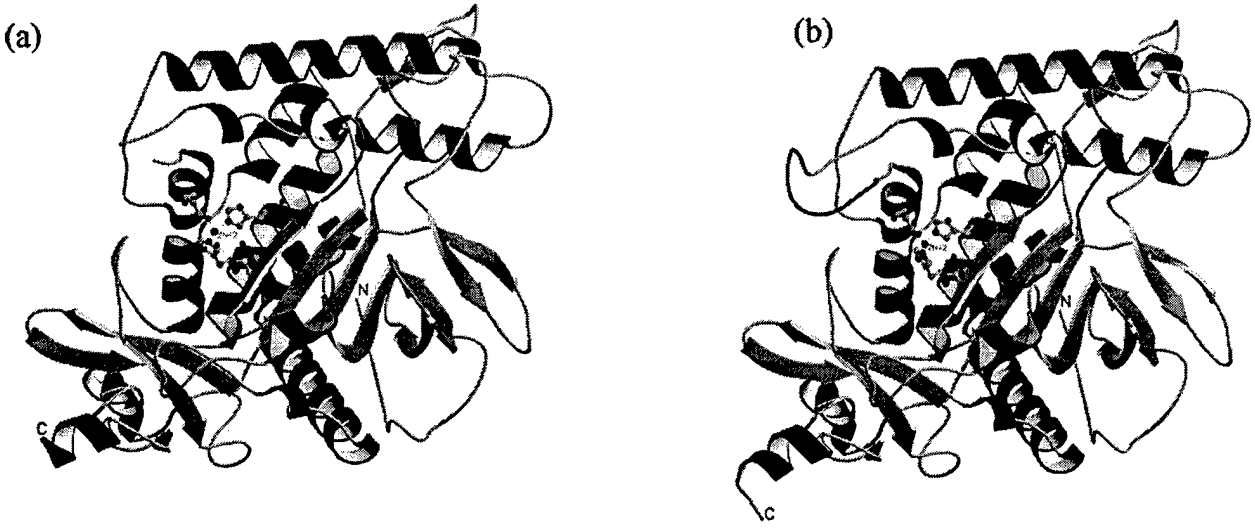

FIGURE 3: Ribbons representation of one monomer of (a) BoNT/E-LC and (b) the mutant Glu212Gln, with zinc and the coordinating residues shown as a ball-and-stick model. The loop region 234−244, which is ordered in the mutant, is shown in brown, while it is missing in the wild type. A few more C-terminal residues were modeled in the mutant than in the wild type.

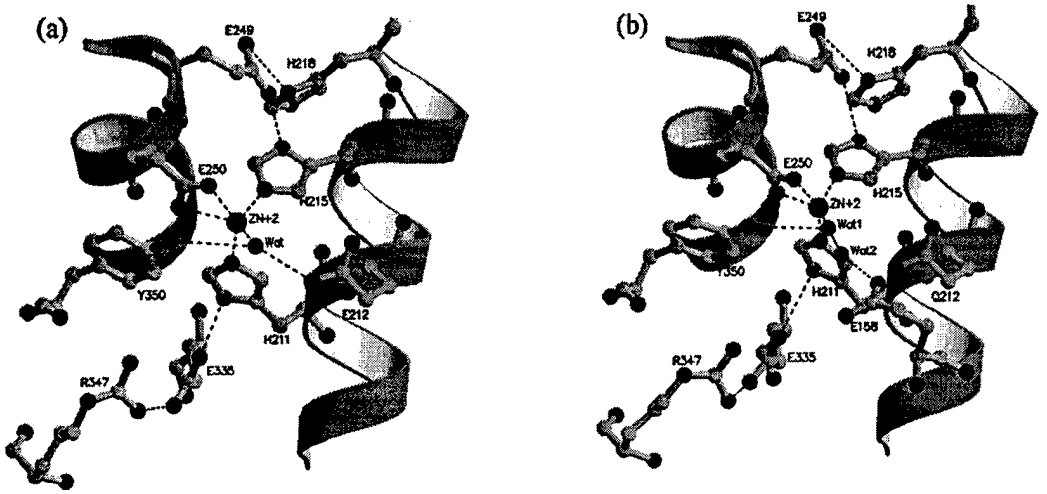

FIGURE 4: Interactions and hydrogen-bonding scheme of relevant residues which are conserved in BoNT/A, /B, and /E LCs. Hydrogen bonds are shown as dashed lines in red. (a) BoNT/E-LC and (b) the mutant Glu212Gln. The water molecule labeled "Wat1" in (b) corresponds to the nucleophilic water but has no hydrogen-bonding interaction with Gln 212.

Table 2. Relevant Interactions (Å) in BoNT/A, /B, and /E and the Mutant Glu212Gln[a]

	BoNT/ E-LC	mutant E212Q	BoNT/ A-LC	BoNT/ B-LC
Zn−H211 NE1	2.18	2.05	2.23	2.11
Zn−H215 NE2	2.16	2.20	2.22	2.15
Zn−E250 OE1	2.22	2.03	2.35	2.60
Zn−E250 OE2	2.46	2.83	2.64	2.20
Zn−Nu. water	2.17	2.79	2.75*	2.08
Nu. water−E212OE1	4.03	4.49	3.42*	3.54
Nu. water−E212OE2	2.86	3.46[b]	2.74*	2.80
Nu. water−Y350-OH	3.58	3.37	10.20*	4.62
Nu. water−E250 OE1	3.15	3.88	4.87*	3.11
Nu. water−R347NH2	7.06	6.92	7.40*	7.46
E335OE1−H211ND1	2.61	2.56	2.66	2.71
E335OE2−R347NH1	2.99	3.19	5.08	3.04
E249OE1−H215ND1	2.76	2.76	3.33	3.03
E249OE1−H218ND1	2.73	2.86	2.92	2.73
Y350-OH−Zn	3.94	3.95	8.10	4.3
Y350-OH−E250OE1	3.15	3.50	5.78	3.69
Y350-OH−E250OE2	3.43	3.30	6.53	3.70
R347NH−Zn	7.08	7.18	7.30	6.5

[a] The numbering scheme in the first column corresponds to BoNT/E. The numbers might vary for other LCs but the amino acids are conserved. In BoNT/A-LC the nucleophilic water (Nu. water) is displaced by Tyr 249 O and marked by an asterisk (*). [b] NE2.

water and the zinc. However, in BoNT/A-LC the corresponding tyrosine residue is farther away from the nucleophilic water. This discrepancy may be due to the autocatalytic nature of BoNT/A-LC, since the peptide bond between Tyr 249 and Tyr 250 is cleaved, as seen in the crystal structure, and positioning of Tyr 249 near the active site might have caused steric problem for Tyr 350 (*22*, *23*). Accordingly, the conserved residues Arg 347 and Tyr 350 may also play similar roles in all serotypes. Mutating residues corresponding to Arg 347 and Tyr 350 reduced the catalytic activity in BoNT/A (*24*) but did not completely abolish the activity. In the same study, it was shown that mutating residue corresponding to Glu 335 (Glu 350 in BoNT/A) drastically reduced the proteolytic activity (*24*). Since the interactions are identical in all serotypes, the effect of mutating these residues in BoNT/E will be the same. We have also shown that Glu 212 Gln completely abolishes the activity, similar to what was observed in BoNT/A (*25*). However, other residues in this sphere and beyond are not conserved and may be responsible for the specificity and selectivity of the toxins. In addition to coming close to zinc and the nucleophilic water, Tyr 350 is only 3.15 Å away from Glu 250 OE1. The interactions between the side-chain carboxylate of Glu 250 and the phenyl ring atoms of Tyr 350 could be characterized as aromatic−anion interactions (*26*). These interactions and the interaction of the hydroxyl group with the nucleophilic water might be stabilizing the side-chain orientation of Glu 250 and the transition state. Loss of this interaction may be one reason why the activity is decreased when Tyr 350 is mutated.

(b) Mutant BoNT/E-LC (Glu212Gln). The crystal structure of the mutant is very similar to the wild-type structure (Figure 3b). Overall, there is no conformational change, and the secondary structural elements are the same. The electron density for 234−244, which was weak in the wild-type structure, was continuous and well defined in the mutant structure. The only difference between the wild type and the mutant is the substitution of Glu with Gln at 212. Though the side-chain orientations of Gln and Glu are very similar, there is no hydrogen-bonding interaction with Gln 212 OE1 or NE2 (distances >3.5 Å), thereby increasing the distance between zinc and the nucleophilic water to 2.8 Å from 2.2 Å in the wild type (Figure 4). This water molecule (which is not a nucleophilic water anymore) is stabilized by a network of water molecules leading up to Glu 158. The charge distribution at the active sites of both wild-type and mutant structures is presented in Figure 6. Since there is no change in the structural features, the inductive effects exerted by the carboxylate side chain of Glu 212 in the wild-type L chain on neighboring groups must be responsible for the pronounced negative surface charge in the periphery of the active site. In other words, the neutralizing effect of the amide group of Gln 212 may be responsible for the decreased negative surface charge. In any case, it is evident that the change in the charge on Glu/Gln disturbs the electrostatic properties of the molecule at the active site, inactivating the toxin.

```
BoNT/B   RRVPLEEFNTNIASVTVNKLISNPGEVERKKGIFANLIIFGPGPVLNENETIDIGIQN-H 179
BoNT/E   DNTPDNQFHIGDASAVEIKFSNGSQDI-----LLPNVIIMGAEPDLFETNSSNISLRNNY 170
BoNT/A   STIDTELKVIDTNCINVIQPDGSYRSE------ELNLVIIGPSADIIQFECKSFGHEVLN 173

BoNT/B   FASREGFGGIMQMKFCPEYVSVFNNVQENKGASIFNRRGYFSDPALILMHELIHVLHGLY 239
BoNT/E   MPSNHGFGSIAIVTFSPEYSFRFNDNSMN---------EFIQDPALTLMHELIHSLHGLY 221
BoNT/A   LTRN-GYGSTQYIRFSPDFTFGFEESLEVDTNPLLGAGKFATDPAVTLAHELIHAGHRLY 232

BoNT/B   GIK-VDDLPIVPNEKKFFMQSTDA-IQAEELYTFGGQDPSIITPSTDKSIYDKVLQNFRG 297
BoNT/E   GAKGITTKYTITQKQNPLITNIRG-TNIEEFLTFGGTDLNIITSAQSNDIYTNLLADYKK 280
BoNT/A   GIAINPNR-VFKVNTNAYYEMSGLEVSFEELRTFGGHDAKFIDSLQENEFRLYYYNKFKD 291

BoNT/B   IVDRLNKVLVCISD-PNININIYKNKFKDKYKFVEDSEGKYSIDVESFDKLYKSLMFGFT 356
BoNT/E   IASKLSKVQVSNP-----LLNPYKDVFEAKYGLDKDASGIYSVNINKFNDIFK-KLYSFT 334
BoNT/A   IASTLNKAKSIVGT--TASLQYMKNVFKEKYLLSEDTSGKFSVDKLKFDKLYKMLTEIYT 349

BoNT/B   ETNIAENYKIKTRASYFSDSLPPVKIKNLLDNEIYTIEEGFNISDKDMEKEYRGQNKAIN 416
BoNT/E   EFDLATKFQVKCRQTYIG-QYKYFKLSNLLNDSIYNISEGYNINN--LKVNFRGQNANLN 391
BoNT/A   EDNFVKFFKVLNRKTYLNFDKAVFKIN-IVPKVNYTIYDGFNLRNTNLAANFNGQNTEIN 408
```

FIGURE 5: Sequence comparison of residues of BoNT/A, /B, and /E (only part of the sequence of LC is shown). The conserved residues are shaded in gray, and residues coordinated to zinc are in boxes. Arg 347 and Tyr 350, presumably involved in transition-state stabilization, are in bold. The underlined residues fall within a sphere of 10-Å radius centered on the active-site zinc. Other residues involved in the catalytic pathway and shown in Figure 7 are shown in white against a black background.

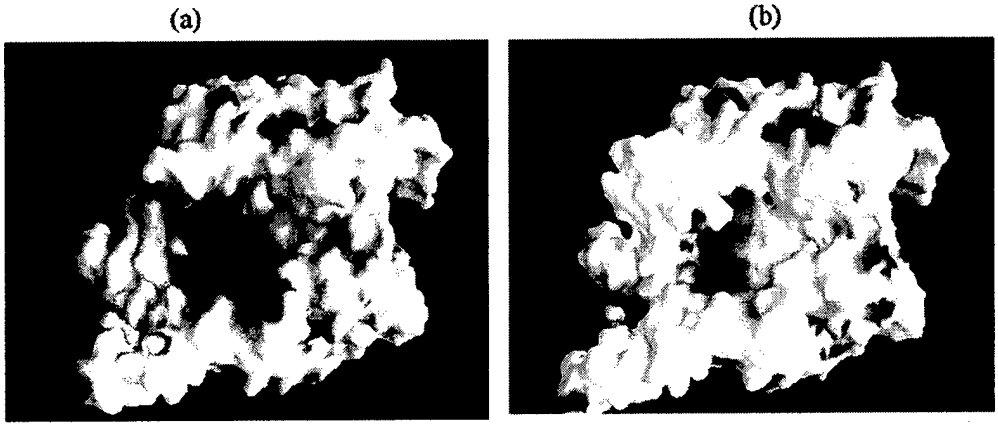

FIGURE 6: Electrostatic potential surfaces of (a) BoNT/E-LC and (b) the mutant Glu212Gln. The positive and negative electrostatic potentials are represented in blue and red. The active site in the wild type is highly negative compared to that in the mutant. In the mutant (b), the active site is partly covered by the loop 234−244 (top left of the figure), which is missing in the wild type.

Since it has been shown in BoNT/A-LC that mutating residues corresponding to Arg 347 and Tyr 350 only reduces but does not completely abrogate the activity, they may not play a major role in the catalytic activity but play a role in stabilizing the transition state. Also, the reduction of the K_{cat} value is much more when Arg 347 is mutated than for Tyr 350 mutation, implying that Tyr 350 plays a less critical role for transition-state stabilization than Arg 347. In any case, they may not act as proton donor for the leaving amide group, in which case the activity would have been lost completely (*24*). However, as we have shown here for BoNT/E-LC, the activity is completely lost when Glu 212 is changed to Gln 212, as in the case of BoNT/A-LC (*25*). These observations, taken together with the movement of nucleophilic water, gives a model for the catalytic activity and the importance of the nucleophilic water and Glu 212. It is evident that Glu 212 helps the leaving group by transferring/shuttling two protons from the nucleophilic water. Our model here is consistent with what we had proposed for BoNT/B (Figure 7) (*27*). The carbonyl oxygen of the scissile bond is polarized by the nucleophilic water, which moves closer to Glu 212 but still maintains its interaction with zinc. The transition tetrahedral state of the carbonyl carbon is stabilized by Arg 347 and Tyr 350. Protons are shuttled to the leaving group in two stages. This scenario is slightly at variance with that proposed for TeNT, where the corresponding tyrosine is suggested to be the proton donor (*28*). It may be that the scheme is somewhat different for TeNT from BoNTs.

Three loops were identified in BoNT/B-LC to have changed conformation when the LC separates from the heavy chain (*8*). Though we see possible changes in conformations of these loops, the extent of the changes seems to be less. When BoNT/A, /B, and /E LCs are compared, loop 50 in BoNT/A-LC seems to take a different conformation. However, this region is not well defined in the electron density map. A direct comparison of loop 250 could not be made since the loop is cleaved in the BoNT/A-LC structure (Figure 8).

This study supports the fact that substitution of the Glu 212 by Gln 212 in the active site leads to the loss of the enzymatic activity of the protein. Structural data suggest that the loss in activity of the protein is not the result of folding

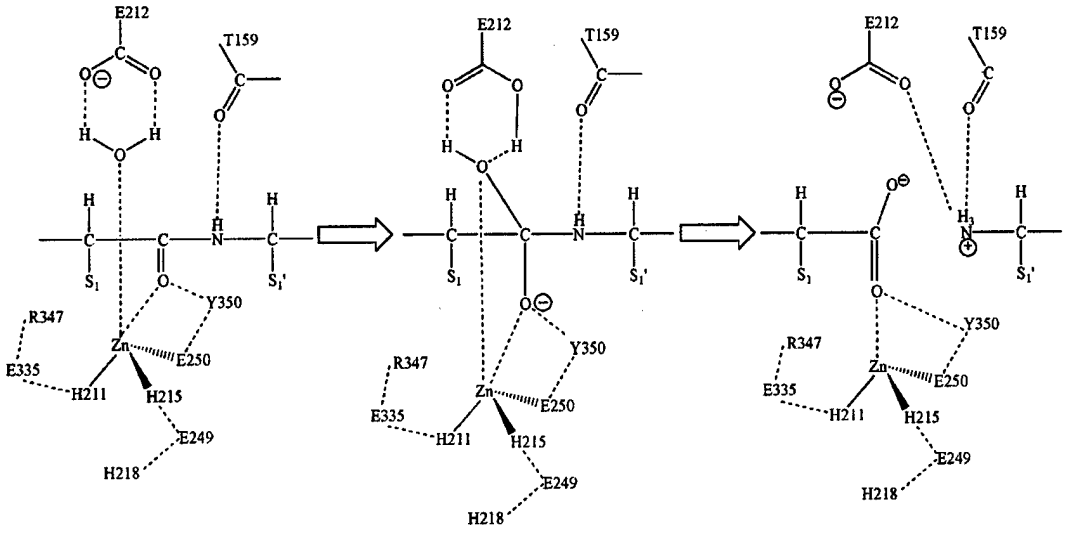

FIGURE 7: Catalytic pathway model for BoNT/E-LC based on our present and previous results. Glu 212 serves as a general base for the catalytic activity and shuttles two protons to the leaving group. His 218, Glu 249, Glu 335, Arg 347, and Tyr 350, stabilizing the orientation of the histidines or the transition state, are also shown, along with Thr 159. While experimental evidence for the role of Glu 249 and His 218 is not yet available, Thr 159 is included here in analogy with our work on BoNT/B (*27*). S1 and S1′ are Arg 180 and Ile 181 of SNAP-25. Hydrogen-bonding interactions and anion−aromatic interactions (Tyr 350−Glu 250) are shown by dashed lines.

FIGURE 8: Stereographic view of a comparison of C-α traces of BoNT/A (green), /B (red), and /E (blue). Except for the loop regions, the conformations are similar.

variation but rather is due to the close involvement of the negative charge of the carboxylate group which directly participates in the hydrolysis of the substrate. The distance and the topographical positioning of the carboxylate group play essential roles in the substrate hydrolysis.

CONCLUSIONS

The present study reveals the role of the nucleophilic water and the charge on Glu212 on the catalytic activity. It also provides a method for developing a novel genetically modified protein vaccine. It suggests that a sensitive inhibitor could be developed if Glu212 is blocked or covalently modified and may well become a common drug for all serotypes. Since the conformation of the mutant is almost identical to that of the wild-type protein and it effectively binds to the substrate, the mutant offers itself as a candidate for studying the enzyme−substrate complex without the substrate being cleaved.

ACKNOWLEDGMENT

We thank Dr. A. Saxena for providing beam time on X12C of the National Synchrotron Light Source, Brookhaven National Laboratory, J. Romeo for technical assistance, and Drs. J. J. Dunn and C. B. Millard for helpful discussions. T.B. was supported by a grant from the Deutsche Forschungsgemeinschaft. A small gift from Allergan, USA, is gratefully acknowledged.

REFERENCES

1. Schiavo, G., Matteoli, M., and Montecucco, C. (2000) Neurotoxins affecting neuroexocytosis, *Physiol. Rev. 80*, 717−766.
2. Schiavo, G., Santucci, A., Dasgupta, B. R., Metha, P. P., Jontes, J., Benfenati, F., Wilson, M. C., and Montecucco, C. (1993) Botulinum neurotoxins serotypes A and E cleave SNAP-25 at distinct COOH-terminal peptide bonds, *FEBS Lett. 335*, 99−103.
3. Binz, T., Blasi, J., Yamasaki, S., Baumeister, A., Link, E., Sudhof, T. C., Jahn, R., and Niemann, H. (1994) Proteolysis of SNAP-25 by Types E and A botulinum neurotoxins, *J. Biol. Chem. 269*, 1617−1620.

4. Vaidyanathan, V. V., Yoshino, K., Jahnz, M., Dorries, C., Bade, S., Nauenburg, S., Niemann, H., and Binz, T. (1999) Proteolysis of SNAP-25 isoforms by botulinum neurotoxin types A, C, and E: Domains and amino acid residues controlling the formation of enzyme−substrate complexes and cleavage, *J. Neurochem. 72*, 327−337.
5. Montecucco, C., and Schiavo, G. (1995) Structure and function of tetanus and botulinum neurotoxins, *Q. Rev. Biophys. 28*, 423−472.
6. Lacy, D. B., Tepp, W., Cohen, A. C., DasGupta, B. R., and Stevens, R. C. (1998) Crystal structure of botulinum neurotoxin type A and implications for toxicity, *Nat. Struct. Biol. 5*, 898−902.
7. Swaminathan, S., and Eswaramoorthy, S. (2000) Structural analysis of the catalytic and binding sites of *Clostridium botulinum* neurotoxin B, *Nat. Struct. Biol. 7*, 693−699.
8. Hanson, M. A., and Stevens, R. C. (2000) Cocrystal structure of synaptobrevin-II bound to botulinum neurotoxin type B at 2.0 A resolution, *Nat. Struct. Biol. 7*, 687−692.
9. Umland, T. C., Wingert, L. M., Swaminathan, S., Furey, W. F., Schmidt, J. J., and Sax, M. (1997) Structure of the receptor binding fragment H_c of tetanus neurotoxin, *Nat. Struct. Biol. 4*, 788−792.
10. Emsley, P., Fotinou, C., Black, I., Fairweather, N. F., Charles, I. G., Watts, C., Hewitt, E., and Isaacs, N. W. (2000) The structures of the H(C) fragment of tetanus toxin with carbohydrate subunit complexes provide insight into ganglioside binding, *J. Biol. Chem. 275*, 8889−8894.
11. Agarwal, R., Eswaramoorthy, S., Kumaran, D., Dunn, J. J., and Swaminathan, S. (2004) Cloning, high level expression, purification and crystallization of the full length Clostridium botulinum neurotoxin type E light chain, *Protein Expr. Purif. 34*, 95−102.
12. Vagin, A., and Teplyakov, A. (2000) An approach to multi-copy search in molecular replacement, *Acta Crystallogr. D56*, 1622−1624.
13. Otwinowski, Z., and Minor, W. (1997) Processing of X-ray diffraction data collected in oscillation mode, *Methods Enzymol. 276*, 307−326.
14. Furey, W., and Swaminathan, S. (1997) PHASES-95: A program package for the processing and analysis of diffraction data from macromolecules., *Methods Enzymol. 276*, 590−620.
15. De La Fortelle, E., and Bricogne, G. (1997) Maximum-likelihood heavy atom parameter refinement in the MIR and MAD methods, *Methods Enzymol. 276*, 472−493.
16. Cowtan, K. (1994) *Joint CCP4 ESF-EACBM Newsl. Protein Crystallogr. 31*, 34−38.
17. Perrakis, A., Morris, R., and Lamzin, V. S. (1999) Automated protein model building combined with iterative structure refinement, *Nat. Struct. Biol. 6*, 458−463.
18. Brunger, A. T., Adams, P. D., Clore, G. M., Delano, W. L., Gros, P., Grosse-Kunstleve, R. W., Jiang, J. S., Kuszewski, J., Nilges, M., Pannu, N. S., Read, R. J., Rice, L. M., Somonsom, T., and Warren, G. L. (1998) Crystallography & NMR system: a new software suite for macromolecular structure determination, *Acta Crystallogr. D54*, 905−921.
19. Laskowski, R. A., MacArthur, M. W., Moss, D. S., and Thornton, J. M. (1993) PROCHECK: a program to check the stereochemical quality for assessing the accuracy of protein structures, *J. Appl. Crystallogr. 26*, 283−291.
20. Washbourne, P., Pellizzari, R., Baldini, G., Wilson, M. C., and Montecucco, C. (1997) Botulinum neurotoxin A and E require the SNARE motif in SNAP-25 for proteolysis, *FEBS Lett. 418*, 1−5.
21. Rigoni, M., Caccin, P., Johnson, E. A., Montecucco, C., and Rossetto, O. (2001) Site-directed mutagenesis identifies active-site residues of the light chain of botulinum neurotoxin type A, *Biochem. Biophys. Res. Commun. 288*, 1231−1237.
22. Ahmed, S. A., and Smith, L. A. (2000) Light chain of botulinum A neurotoxin expressed as an inclusion body from a synthetic gene is catalytically and functionally active, *J. Protein Chem. 19*, 475−487.
23. DasGupta, B. R., and Foley, J. (1989) C. Botulinum neurotoxin types A and E: isolated light chain breaks down into two fragments. Comparison of their amino acid sequences with tetanus neurotoxin, *Biochemie 71*, 1193−1200.
24. Binz, T., Bade, S., Rummel, A., Kollewe, A., and Alves, J. (2002) Arg^{362} and Tyr^{365} of the botulinum neurotoxin type A light chain are involved in transition state stabilization, *Biochemistry 41*, 1717−1723.
25. Li, L., Binz, T., Niemann, H., and Singh, B. R. (2000) Probing the mechanistic role of glutamate residues in the zinc-binding motif of type A botulinum neurotoxin light chain, *Biochemistry 39*, 2399−2405.
26. Jalbout, A. F., and Adamowicz, L. (2002) Anion-aromatic molecule complex. *Ab initio* study of the benzene.O_2 anion, *J. Chem. Phys. 116*, 9672−9676.
27. Swaminathan, S., Eswaramoorthy, S., and Kumaran, D. (2004) Structure and enzymatic activity of botulinum neurotoxins, *Mov. Disord. 19* (Suppl. 8), S17−S22.
28. Rossetto, O., Caccin, P., Rigoni, M., Tonello, F., Bortoletto, N., Stevens, R. C., and Montecucco., C. (2001) Active-site mutagenesis of tetanus neurotoxin implicates TYR-375 and GLU-271 in metalloproteolytic activity, *Toxicon 39*, 1151−1159.

BI036278W